Hepatitis B Virus Evasion From Cyclic Guanosine Monophosphate-Adenosine Monophosphate Synthase Sensing in Human Hepatocytes

Eloi R Verrier, Seung-Ae Yim, Laura Heydmann, Houssein El Saghire, Charlotte Bach, Vincent Turon-Lagot, Laurent Mailly, Sarah C Durand, Julie Lucifora, David Durantel, et al.

Hepatitis B virus evasion from cGAS sensing in human hepatocytes

Eloi R. Verrier[1,$,*], Seung-Ae Yim[1,$], Laura Heydmann[1], Houssein El Saghire[1], Charlotte Bach[1], Vincent Turon-Lagot[1], Laurent Mailly[1], Sarah C. Durand[1], Julie Lucifora[2], David Durantel[2], Patrick Pessaux[1,3], Nicolas Manel[4,5], Ivan Hirsch[6], Mirjam B. Zeisel[1], Nathalie Pochet[7], Catherine Schuster[1,#,*] and Thomas F. Baumert[1,3,#,*]

[$]ERV and SAY contributed equally as first authors, alphabetical order.

[#]CS and TFB contributed equally as senior authors

[1]Université de Strasbourg, Inserm, Institut de Recherche sur les Maladies Virales et Hépatiques UMRS 1110, F-67000 Strasbourg, France; [2]Inserm, U1052, Cancer Research Center of Lyon (CRCL), Université de Lyon (UCBL1), CNRS UMR_5286, Centre Léon Bérard, Lyon, France; [3]Pôle Hépato-Digestif, Institut Hospitalo-Universitaire, Hôpitaux Universitaires de Strasbourg, F-67000 Strasbourg, France; [4]Immunity and Cancer Department, Institut Curie, PSL Research University, F-75005 Paris, France; [5]Inserm, U932, F-75005 Paris, France; [6]Department of Genetics and Microbiology, Faculty of Science, Biocev, Charles University, 12844 Prague, Czech Republic; Institute of Organic Chemistry and Biochemistry, CAS, IOCB & Gilead Research Center, 16610 Prague, [7]Ann Romney Center for Neurologic Diseases, Department of Neurology, Brigham and Women's Hospital, Harvard Medical School, Boston, MA 02115, USA, Cell Circuits Program, Broad Institute of MIT and Harvard, Cambridge, MA 02142, USA.

***Corresponding authors**: Prof. Thomas F. Baumert, MD, e-mail: thomas.baumert@unistra.fr, Dr. Catherine Schuster, PhD, e-mail: catherine.schuster@unistra.fr, and Dr. Eloi R. Verrier, PhD, e-mail: e.verrier@unistra.fr, Inserm U1110, Institut de Recherche sur les Maladies Virales et Hépatiques, 3 Rue Koeberlé, 67000 Strasbourg, France. Tel: +33 3 68 85 37 03; fax: +33 3 68 85 37 24.

Key words antiviral, capsid, innate immunity, liver, recognition.

List of Abbreviations

HBV: hepatitis B virus; cGAS: cyclic GMP-AMP synthase; HSPG: heparan sulfate proteoglycan; NTCP: Na+/taurocholate cotransporting polypeptide; rcDNA: relaxed circular DNA; cccDNA: covalently closed circular DNA; pgRNA: pregenomic RNA; PRR: pattern recognition receptors; cGAMP: cyclic GMP-AMP; IFN: interferon; STING: stimulator of IFN genes; ISG: IFN-stimulated gene; PHH: primary human hepatocyte; PEG: polyethylene glycol; siRNA: small interfering RNA; HIV: human immunodeficiency virus; VSV-G: vesicular stomatitis virus glycoprotein; sgRNA: single-guide RNA; PMM: primary hepatocyte maintenance medium; dslDNA: double stranded linear DNA; dsDNA: double stranded DNA; GSEA: gene set enrichment analysis; FDR: false discovery rate; FISH: fluorescence in situ hybridization; KO: knock-out. SeV: Sendai virus. IAR: innate antiviral response gene set. Dpi: days post infection.

Financial support: This work was supported by the European Union (ERC-AdG-2014-671231-HEPCIR, EU H2020-667273-HEPCAR, EU-InfectEra HepBccc), the National Institute of Health (NIAID 1R03AI131066-01A1, NCI R21 CA209940 and NIAID U19AI123862), the Agence Nationale de Recherches sur le Sida et les Hepatites Virales (ANRS, 2015/1099), the Fondation ARC pour la Recherche sur le Cancer (TheraHCC IHUARC IHU201301187), GACR 17-15422S, and a PhD fellowship of the Région Alsace, France. The work has been published under the framework of the LABEX ANR-10-LABX-0028_HEPSYS and benefits from funding from the state managed by the French National Research Agency as part of the Investments for the future program. E.R.V. was supported by an ANRS fellowship (ECTZ50121).

Abstract

Chronic hepatitis B virus (HBV) infection is a major cause of chronic liver disease and cancer worldwide. The mechanisms of viral genome sensing and the evasion of innate immune responses by HBV infection are still poorly understood. Recently, the cyclic GMP-AMP synthase (cGAS) was identified as a DNA sensor. In this study, we aimed to investigate the functional role of cGAS in sensing of HBV infection and elucidate the mechanisms of viral evasion. We performed functional studies including loss- and gain-of-function experiments combined with cGAS effector gene expression profiling in an infectious cell culture model, primary human hepatocytes and HBV-infected human liver chimeric mice. Here we show that cGAS is expressed in the human liver, primary human hepatocytes and human liver chimeric mice. While naked relaxed-circular HBV DNA is sensed in a cGAS-dependent manner in hepatoma cell lines and primary human hepatocytes, host cell recognition of viral nucleic acids is abolished during HBV infection, suggesting escape from sensing, likely during packaging of the genome into the viral capsid. While the hepatocyte cGAS pathway is functionally active, as shown by reduction of viral cccDNA levels in gain-of-function studies, HBV infection suppressed cGAS expression and function in cell culture models and humanized mice. ***Conclusion***: HBV exploits multiple strategies to evade sensing and antiviral activity of cGAS and its effector pathways.

With more than 250 million chronically infected patients, hepatitis B virus (HBV) infection is a leading cause of liver disease and hepatocellular carcinoma (1, 2). Current antiviral therapies effectively control viral load, but largely fail to cure (3). HBV is a partially double stranded DNA (dsDNA) virus infecting human hepatocytes after initial attachment to heparan sulfate proteoglycans (HSPG) and its receptor Na+/taurocholate cotransporting polypeptide (NTCP; reviewed in (4)). Following uncoating, the viral nucleocapsid is released into the cytoplasm. The viral genome is imported into the nucleus through mechanisms which are still poorly understood. The viral genome it is converted in the nucleus into a covalently closed circular DNA (cccDNA) (5). This minichromosome serves as a template for both pregenomic RNA (pgRNA) and viral mRNA transcription. While recent studies suggested sensing of the pgRNA or other HBV RNAs by either MDA5 (6) or RIG-I (7), the recognition of the viral nucleic acids by the regular pattern recognition receptors (PRRs) still remains elusive. In general, HBV does not or only marginally activate innate immune responses in cell culture models and *in vivo* (8-14), leading to the concept that HBV behaves like a “stealth” virus avoiding viral DNA and RNA sensing (15). Other studies have suggested an active inhibition of the innate immune responses by HBV proteins (16). Consequently, the interaction of HBV and the innate immune system of hepatocytes, and in particular the sensing of HBV DNA, is only poorly understood.

Foreign DNA recognition by cytosolic DNA sensors triggers an early antiviral innate immune response, including type I and type III IFN production (17). Recently, the cyclic GMP-AMP (cGAMP) synthase (cGAS) was identified as a DNA sensor exhibiting an antiviral activity against a broad range of DNA and RNA viruses (18-20). cGAS is encoded by *MB21D1* gene and directly binds to dsDNAs inducing the production of cGAMP which is recognized by the stimulator of IFN genes (STING, encoded by *TMEM173*) triggering the expression of IFN-stimulated genes (ISGs) through TBK1 activation (21-23). While two studies have investigated cGAS-HBV

interactions in viral replication and assembly (24, 25), the functional role of cGAS in sensing of the viral genome during natural infection of human hepatocytes remains unknown.

The understanding of HBV-host interactions, including innate immune response after infection, has been hampered for long time by the absence of robust cell culture model system for the study of viral infection (26). The development of HBV-susceptible NTCP-overexpressing hepatoma cells, such as HepG2-NTCP cells, allows the study of the full life cycle in a robust and easy-to-use cell culture model (26). HepG2 cells are capable of mounting an efficient innate immune response after infection by hepatitis C virus (27). Moreover, another study took advantage of HBV-infected HepG2-NTCP for studying the interaction between RIG-I and HBV RNA (7), suggesting that this cell line is suitable for the study of innate immune response after HBV infection. Here, we aimed to understand the functional role of cGAS for the HBV life cycle in human hepatocytes and unravel the mechanisms of viral evasion using loss- and gain-of-function experiments combined with cGAS effector gene expression profiling in human liver chimeric mice.

EXPERIMENTAL PROCEDURES

Human subjects. Human material including liver tissue from patients undergoing surgical resection or HBV-positive serum was obtained with informed consent from all patients. Protocols were approved by the Ethics Committee of the University of Strasbourg Hospitals, France (CPP 10-17 and DC-2016-2616).

Animal Experimentation. All mice were kept in a specific pathogen-free animal housing facility at Inserm U1110. The respective protocols were approved by the Ethics Committee of the University of Strasbourg Hospitals and authorized by the French Ministry of Research (number 02014120416254981AL/02/19/08/12, AL/01/18/08/1202014120416254981, 0201412051105

4408). Mice were kept in individual ventilated cages, with bedding composed of irradiated sawdust and chips from spruce and pine and enriched with cotton cocoon and aspen bricks. The animal diet consists of 25kGy irradiated RM3(E) (SDS) and mice were not fasted. Primary human hepatocytes (PHH) were transplanted into 3 week-old uPA/SCID-bg mice (male and female) by intrasplenic injection as described (28). Engraftment and viability of PHH were assessed by quantification of human serum albumin by ELISA (E80-129, Bethyl Laboratories; (28)). uPA/SCID-bg mice were then infected with serum-derived HBV and sacrificed 16 weeks after virus inoculation. Serum HBV load was determined by qPCR (Realtime HBV viral load kit, Abbott) before sacrifice. Interventions were all performed during light cycle.

Cell lines and human hepatocytes. HEK 293T (29) and HepG2-NTCP (30) cells and isolation of PHH have been described (29).

Reagents and plasmids. DMSO, PEG 8000 (polyethylene glycol), Poly (I:C) and calf thymus DNA (control dsDNA) were obtained from Sigma-Aldrich, pReceiver-Lv151 plasmid from GeneCopoeia™ and lentiCas9-Blast and lentiGuide-Puro plasmids were gifts from Feng Zhang (Addgene #52962 and #52963).

Small interfering RNAs for functional studies. Pools of ON-TARGET plus (Dharmacon) small interfering RNA (siRNA) targeting *MB21D1* (cGAS), *TMEM173* (STING), *TBK1*, and *IFI16* expression were reverse-transfected into HepG2-NTCP using Lipofectamine RNAi-MAX (Invitrogen) as described (29). RNA was purified from cells harvested two days after transfection and gene expression was analyzed using qRT-PCR.

HepG2-NTCP-cGAS overexpressing and *MB21D* knock-out cells. Lentivirus particles were generated in HEK 293T cells by cotransfection of plasmids expressing the human immunodeficiency virus (HIV) gap-pol, the vesicular stomatitis virus glycoprotein (VSV-G) and either the human *MB21D1* full open reading frame (ORF) encoding plasmid, or the *MB21D1*-targeting single-guide RNA (sgRNA) encoding plasmids, or the Cas9 expressing plasmid in the ratio of 10:3:10. HepG2-NTCP cells were then plated and transduced with lentivirus encoding either the human *MB21D1* ORF or the *eGFP* ORF in pReceiver-Lv151 vector (GeneCopoeia™). After 3 days, transduced cells were selected with 200 µg/ml of neomycin (G418). The cGAS-over-expressing and control HepG2-NTCP cells were then further cultured in presence of G418 at 200 µg/ml. For the generation of *MB21D1* knock-out cell lines, one *MB21D1*-targeting sgRNA was designed using CRISPR Design Tool (Broad Institute: http://www.genome-engineering.org/crispr/?page_id=41). The sgRNA sequence targeting the exon 1 of *MB21D1* (sgcGAS 5'-CACCGCGGCCCCCATTCTCGTACGG-3') was inserted into lentiGuide-Puro plasmid (31). We first generated Cas9 expressing HepG2-NTCP cells after transduction of cells with the lentiCas9-Blast plasmid (31). Cells were then selected with 6 µg/ml blasticidin for 10 days. HepG2-NTCP-Cas9 cells were seeded in six-well plates at 50% confluency 24 h prior to transduction with the sgcGAS-encoding plasmid. Subpopulations of cells were selected from the whole population and cultured independently. cGAS expression was controlled by Western blot. Finally, two cGAS-deficient cell lines (cGAS_KO#1 and cGAS_KO#2) were selected.

Analysis of gene expression using qRT-PCR. Total RNA was extracted using ReliaPrep™ RNA Miniprep Systems (Promega) and reverse transcribed into cDNA using Maxima First Strand cDNA Synthesis Kit (Thermo Scientific) according to the manufacturer's instructions. Gene expression was then quantified by qPCR using a CFX96 thermocycler (Bio-Rad). Primers and TaqMan®

probes for *MB21D1* (cGAS), *TMEM173* (STING), *TBK1*, *IFI16*, *IFNB1*, *IFNL1,* and *GAPDH* mRNA detection were obtained from ThermoFisher (TaqMan® Gene expression Assay, Applied Biosystems). All values were normalized to *GAPDH* expression.

Protein expression. The expression of cGAS, STING, and β-actin proteins was assessed by Western blot as described (30) using two polyclonal rabbit anti-cGAS antibodies (HPA031700, Sigma & NBP1-86761, Novus Biologicals, see Supporting Information), a polyclonal rabbit anti-STING antibody (19851-1-AP, Proteintech), and monoclonal anti-β-actin antibody (mAbcam8226, Abcam). Protein expression was quantified using ImageJ software.

Infection of HepG2-NTCP cells and PHH. The purification of infectious recombinant HBV particles from HepAD38 cells and infection of HepG2-NTCP cells has been described (30). Briefly, HepG2-NTCP and derived cells were plated one day prior to incubation with HBV in presence of 4% PEG at multiplicity of infection (MOI) ~ 500 genome equivalent/cell (GEq/cell) except otherwise stated. Sixteen hours after HBV inoculation, cells were washed with PBS and then cultured in 3.5% DMSO primary hepatocyte maintenance medium (PMM) for ten days. HBV infection was assessed by quantification of HBV pgRNA using qRT-PCR or HBV total DNA using qPCR as described (30), or by immunofluorescence (IF) using anti-HBsAg antibody (1044/329, Bio-Techne) and AF647-labelled goat antibody targeting mouse IgGs (115-605-003, Jackson Research) as described (30). Southern blot detection of HBV cccDNA was performed using DIG-labelled (Roche) specific probes as described (32). Total DNA from HBV-infected cells was extracted using the previously described HIRT method (33). Specific DIG-labelled probes for the detection of HBV and mitochondrial DNAs were synthetized using the PCR DIG Probe Synthesis Kit (Roche) and the primers indicated in Table S1. PHH were plated one day prior to incubation

with a HBV preS1- or a control peptide for one hour at 37°C as described (30). PHH were then infected with recombinant HBV particles for ten days. HBV infection was assessed by quantification of HBV pgRNA using qRT-PCR and immunofluorescence as described above.

Sendai virus (SeV) infection. HepG2-NTCP cells and PHH were infected with SeV DI-H4 at an MOI of 10 as described (13).

Extraction of HBV rcDNA from HBV infectious particles. HBV rcDNA was extracted from HBV preparations using QiaAMP DNA MiniKit protocol (Qiagen). PEG-precipitated cell supernatants from naive HepG2-NTCP cells were used as non-virion controls. The presence of HBV DNA was confirmed by PCR and quantified by qPCR as described (30) (see Supporting Information). One µg of rcDNA or dsDNA (calf thymus DNA) was transfected in cells using Lipofectamine 2000 (Invitrogen) and CalPhos Mammalian Transfection Kit (Clonetech) according to manufacturer's instructions. Cells transfected with HepG2-NTCP control supernatants were used as a control. Three days after transfection, total RNA was extracted and purified as described above.

Transcriptomic analysis by digital multiplexed gene profiling using nCounter NanoString. Transcriptomic analyses using nCounter NanoString were performed according to manufacturer's instructions. Specific probes for a set of 36 innate antiviral response-related (IAR) genes (according to (20) and additional genes listed in Table S2) were obtained from the manufacturer. HepG2-NTCP cells, HepG2-NTCP derived cell lines and PHH were either infected with HBV or SeV, or were transfected with Poly (I:C) (100ng) for two days. Alternatively, HepG2-NTCP-Cas9 and HepG2-NTCP-KO_cGAS#2 cells were transfected with rcDNA (1µg) or dsDNA (calf thymus DNA, 1µg) for three days. Total RNA was then extracted and subjected to nCounter Digital

Analyzer system (NanoString). Alternatively, total liver RNA was extracted from HBV-infected mice and gene expression was assessed by either qRT-PCR (*MB21D1* expression) or nCounter Digital Analyzer system. The 36 genes were considered as an artificial gene set termed innate antiviral response (IAR) gene set. Its perturbation by infection, transfection or gain-/loss-of -function studies was assessed through Gene Set Enrichment Analysis (GSEA (34)). GSEA determines whether an a priori defined set of genes shows statistically significant differences between two biological states. False discovery rate (FDR) < 0.05 was considered statistically significant. Heatmaps illustrating the induction (red) or repression (blue) of the genes of the IAR compared to control were illustrated using Morpheus software (Broad Institute of MIT and Harvard, Cambridge, MA, USA). The heatmap illustrating the induction (red) or repression (blue) of individual genes in chimeric mouse livers were designed using GenePattern (Broad Institute of MIT and Harvard, Cambridge, MA, USA).

FISH analyses. Fluorescence in situ hybridization (FISH) analyses were performed as described (28, 35). Briefly, liver samples were collected from mice and then immediately embedded into optimal cutting temperature compound (OCT). OCT-embedded liver sections were cryosectioned (10 µm) using a cryostat (Leica). Upon fixation with 4% formaldehyde at 4°C, washing, and dehydration in ethanol, tissue sections were boiled at 90–95°C for 1 min in a pretreatment solution (Affymetrix-Panomics), followed by a 10 min digestion in protease QF (Affymetrix-Panomics) at 40°C. Sections were then hybridized using specific probe sets targeting HBV (target region nucleotides 483-1473 of HBV [Genotype D, GenBank V01460]) and human *MD21D1* (VA1-3013492-VC, Affymetrix-Panomics). Pre-amplification, amplification and detection of bound probes were performed according to the manufacturer's instructions. Finally, pictures were acquired by LSCM (LSM710, Carl Zeiss Microscopy) and Zen2 software.

Statistical Analysis. Except otherwise stated, cell culture experiments were performed at least three times in an independent manner. Statistical comparisons of the samples were performed using a two-tailed Mann-Whitney U test. For *in vivo* experiments, a two-tailed unpaired Student's t-test was performed for comparing gene expression from non-infected and HBV-infected mice. $p < 0.05$ (*), $p < 0.01$ (**), and $p < 0.001$ (***) were considered significant. Significant p values are indicated by asterisks in the figures. Each digital multiplexed gene profiling experiment was performed using three biological replicates per condition and the induction or repression of the gene set was analyzed using GSEA. FDR < 0.05 was considered statistically significant.

RESULTS

Expression of cGAS in primary human hepatocytes and an infectious HBV cell culture model. Prior to its functional characterization, we studied cGAS/*MB21D1* expression in primary hepatocytes and HBV permissive cell lines. As shown in Figure 1A, cGAS protein expression was easily detectable in PHH from three independent donors. Since HBV infection of primary cells is highly variable and does not allow robust perturbation studies, we used an HBV infectious cell culture model based on differentiated hepatocyte-derived HepG2 cells overexpressing NTCP (30) – a key HBV entry factor. As shown in Figure 1A, cGAS protein is expressed in HepG2-NTCP cells. We validated the specificity of cGAS detection using a siRNA specifically targeting the *MD21B1* expression (sicGAS) and Western blots applying two antibodies (Figure 1A, Figure S1). Moreover, we generated CRISPR-mediated *MB21D1* knock-out (KO) cells using a specific sgRNA (Figure 1B). Two cell lines, KO_cGAS#1 and KO_cGAS#2 were selected for further studies (Figure 1B). Interestingly, the adaptor STING was also detected in HepG2-NTCP cells, suggesting a fully functional cGAS-STING pathway (Figure 1C). To test the suitability of these cells as a

model to analyze cGAS-mediated innate immune response after virus infection, we stimulated cells with different analogs of viral nucleic acids. Stimulation by Poly (I:C) or dsDNA transfection elicited a dose-dependent *IFNB1* expression in HepG2-NTCP cells (Figure 1D). These results suggest that the cGAS sensing machinery is present, functional, even if it is less efficient that the RNA sensing complex. Moreover, cGAS protein expression was induced by both Poly (I:C) and dsDNA stimulation confirming an efficient IFN response through the upregulation of ISGs such as *MB21D1* (36) after RNA or DNA stimulation (Figure 1E). Collectively, these data show that the HepG2-NTCP model is suitable to study innate immune responses.

HBV evades cGAS sensing. Next, we investigated whether HBV was sensed in HBV permissive cells. To address this question, we infected HepG2-NTCP cells with recombinant HBV (MOI: 500 GEq/cell) and studied the expression of *IFNB1* at early time points after HBV infection. As it has been described that HBV infection may induce the expression of type III IFN (7), *IFNL1* expression was also quantified. As shown in Figure 2A-B, the lack of increase in *IFNB1* and *IFNL1* expression in spite of efficient infection (Figure S2) indicates poor or absent detection of HBV by cellular sensors. In contrast, SeV, known to induce a strong IFN response in hepatocytes (13), strongly induced *IFNB1* and *IFNL1* expression (Figure 2 AB). Since cGAS has been shown to induce the expression of a large set of innate effector genes (such as *OAS2* or *IFI44*, see (20)), the analysis of expression of a single effector gene such *IFNB1* may not be sufficient to evaluate cGAS sensing. Therefore, we designed a 36 innate antiviral response gene set (named IAR), comprising 29 ISGs whose expression is modulated by cGAS activity described by Schoggins and Rice in (20) as well as 7 established innate immune response effector genes (Table S2). We then infected HepG2-NTCP cells with HBV or SeV, and measured the innate antiviral immune response at day 2 post infection by analysis of IAR gene expression using digital multiplexed gene profiling

(nCounter NanoString) and GSEA-based analysis. Whereas Poly (I:C) transfection and SeV infection induced a marked modulation of cGAS effector/IAR gene expression (FDR = 0.004 and < 0.001, respectively), no significant modulation of IAR gene expression was observed in HBV-infected cells (Figure 2C), as further illustrated by the expression of *IFNB1* and *IFI44* (Figure 2E). To measure the impact of cGAS expression on cellular response to HBV infection, we then infected cGAS-depleted (KO_cGAS#2) and -overexpressing (cGAS_OE) HepG2-NTCP cells with HBV and analyzed the expression of the cGAS-related genes after infection. As shown in Figure 2D, no significant modulation of the IAR signature was observed in HBV-infected samples, as further illustrated by absent modulation of *IFNB1* and *IFI44* expression (Figure 2F).

To exclude the possibility that low HBV infection could be the reason for the absence of IFN induction, we performed additional experiments using increasing MOIs. As shown in Figure 3A-C, no induction of *IFNB1* (Figure 3A) was observed even at a MOI 10000, despite very high infection efficiency as shown by quantitation of pre-genomic RNA and immunofluorescence of HBsAg (Figure 3B-C). To investigate whether IFN induction occurs potentially at a very early step of viral infection and was missed in the experimental design shown above, we performed a time course studying IFN response to HBV within the first 24 hours post infection. As shown in Figure 3D, HBV infection did not induce a measurable IFN response during early steps of HBV infection. In contrast, SeV, an established inducer of IFN showed robust induction of IFN responses in HepG2-NTCP cells (Figure 3D). Taken together, these data suggest an absence of sensing of HBV infection by the cGAS-STING pathway in HepG2-NTCP cells.

As the HBV genome is packaged into the nucleocapsid (37), we investigated whether packaging shields virion DNA from cGAS recognition. We purified HBV genomic rcDNA from HBV infectious particles (Figure S3) and transfected the naked viral genome into HepG2-NTCP cells (1 µg, corresponding to approximately 10^6-10^7 HBV DNA copies/µL). As shown in Figure 4A, a

significant (FDR = 0.02) induction of the IAR signature (illustrated by *IFNB1* and *IFI44* expression, Figure 4B) was observed after both rcDNA and dsDNA transfection, suggesting sensing of the naked HBV genome. Interestingly, the amount of cellular HBV DNA copies was higher in HBV-infected cells compared to rcDNA transfected cells (Figure 4C), confirming that the levels of HBV DNA in HBV infected cells are sufficient to trigger IFN signaling and the absence of HBV sensing in infected cells was not due to low MOIs. Moreover, the induction of the IAR gene expression was absent in HepG2-NTCP-KO_cGAS#2 cells, suggesting a cGAS-specific activation of innate immunity by both dsDNA and rcDNA transfection in our model.

To validate these observations in a more physiological model, we infected PHH with HBV and control cGAS gene expression after two days of infection. Interestingly, while SeV strongly induced IAR gene expression (Figure 5B), a highly efficient HBV infection (Figure 5A) did not induce the induction of the expression of innate antiviral response genes (Figure 5B). In contrast, the transfection of rcDNA and dsRNA into PHH from four different donors robustly triggered the expression of *IFNB1* and *IFNL1* (Figure 5C), suggesting a robust sensing of viral DNA in human hepatocytes. Collectively, these data suggest that non-encapsidated HBV DNA is sensed by cGAS, but this sensing is impaired during HBV infection.

The cGAS-STING pathway exhibits robust antiviral activity against HBV infection with reduction of cccDNA levels. As cGAS exhibits an antiviral activity against a broad range of DNA and RNA viruses (meaning even in absence of direct viral sensing) (20), we then investigated the antiviral effect of the cGAS-STING signaling pathway in HBV infection. We silenced the expression *MB21D1*, *TMEM173* (encoding the STING protein), *TBK1* and *IFI16* (encoding the gamma-interferon-inducible protein 16, another cytoplasmic DNA sensor able to directly activate STING (17)) in HepG2-NTCP cells prior to infection with HBV. As shown in Figure 6A-B, silencing

of *MB21D1*, *TMEM173* and *TBK1* expression induced a marked increase in HBV infection. In contrast, the silencing of *IFI16* had no effect on HBV infection. CRISPR/Cas9-mediated KO or overexpression of cGAS protein resulted in a marked increase or decrease in HBV infection and HBV cccDNA levels – the key viral nucleic acid responsible for viral persistence (Figure 6C-E). Notably, the overexpression of cGAS did not affect NTCP expression at the cell surface, suggesting that the susceptibilities of the different cell lines to HBV infection are equivalent (Figure S4). Taken together, our results suggest that cGAS is functional and exerts antiviral activity in HBV permissive cells.

HBV infection induces repression of cGAS and its effector gene expression in cell culture and in liver chimeric mice. As several reports have suggested that HBV proteins can inhibit IFN-signaling pathways (16), we next investigated whether HBV infection interferes with the expression of cGAS-related gene by quantifying *MB21D1*/cGAS mRNA and protein expression (Figure 7A-B). Interestingly, cGAS protein expression (Figure 7B) as well as the expression of *MB21D1*, *TMEM173*, and *TBK1* mRNA (Figure 7C) were significantly inhibited in HBV-infected cells. To confirm this observation *in vivo*, we then investigated the expression of human *MB21D1* expression in HBV-infected human liver chimeric mice. *MB21D1* was expressed at low but detectable levels (Figure 7D). As shown in Figure 7E, *MB21D1* expression was significantly (p = 0.013) downregulated in HBV-infected mice compared to non-infected control mice, confirming our results in the cell culture model. Importantly, *MB21D1* expression levels did not correlate with HBV genotype (Table 1). An absent correlation of human serum albumin with either *MB21D1* expression (Table 1, Figure 7E) or status of HBV infection (Table 1, t-test HBV versus Ctrl: p = 0.26) largely excludes that the observed differences in cGAS expression are due to different human hepatocyte repopulation levels or due to a decrease of human hepatocyte cell viability in

individual animals. To investigate whether HBV modulates cGAS effector function, we analyzed virus-induced changes on cGAS effector gene expression using gene expression profiling in three control mice and the three HBV-infected mice exhibiting the lowest levels of *MB21D1* expression (Table 1). As shown in Figure 7F, HBV infection resulted in a significant (FDR = 0.047) down-regulation of the expression of cGAS effector genes in human hepatocytes in chimeric mice. The data showed that HBV represses expression of cGAS and its effector genes *in vivo*.

DISCUSSION

The interaction between HBV and the innate immune system is a complex process still remaining elusive and controversial (15). Collectively, our data demonstrate that in human hepatocytes (i) naked HBV genomic rcDNA is sensed in a cGAS-dependent manner whereas the packaged HBV genome appears not to be recognized during viral infection; (ii) cGAS-STING pathway exhibits antiviral activity against HBV infection including reduction of viral cccDNA levels; (iii) HBV infection suppresses both cGAS expression and function in cell culture and humanized liver chimeric mice.

The detection of HBV DNA by the cellular sensors within infected cells is still poorly understood and remains controversial. *In vitro* and *in vivo* data strongly suggest that HBV behaves like a stealth virus unable to trigger any innate immune response (8, 9, 11). Other studies have suggested that HBV-derived dsDNA fragments (25) and viral nucleocapsid destabilization and disassembly (38, 39) could induce innate immune responses. Our results demonstrate, that in human hepatocytes - the natural target cell of HBV infection - the exposure of the naked HBV genome leads to the activation of innate antiviral immune responses. In contrast, sensing is largely absent during HBV infection, most likely due to packaging into the viral capsid. These results extend a previous observation in hepatoma cell lines transfected with replication-competent HBV DNA that the HBV genome itself can be recognized by the classical sensors (25).

Interestingly, the capsid of HIV-1 also prevents the sensing of HIV cDNA by cGAS following reverse-transcription up to integration, whereas HIV-2 capsid may unmask the cDNA leading to a stronger sensing by cGAS and a lower pathogenicity of the strain (40).

Another explanation of this absence of sensing would be the lack a functional STING protein in hepatocyte, as it has been recently reported (41). In our study, rcDNA and dsDNA were sensed in a cGAS-dependent manner and were able to activate the cGAS-mediated antiviral response in HepG2-NTCP cells (Figure 2). Moreover, we detected STING at the protein level in accordance with a recent study (42) and specific silencing of *TMEM173* (STING) expression was associated with a significant increase in HBV infection (Figure 6). Consequently, it is likely that STING is functionally active in HepG2 cells. The observed HBV DNA sensing in PHH (Figure 5) suggests that the foreign DNA detection pathways are active in PHH as well. This observed innate immune response in spite of a weak STING expression may suggest a STING-independent activity of cGAS as it has been recently reported (43), including in hepatocytes (44). To understand the impact of the cGAS and STING expression on innate immune response to HBV infection, it would be of further interest to analyze the HBV-induced modulation of gene expression in Kupffer cells following phagocytosis, as they exhibit higher STING- and cGAS levels compared to hepatocytes (41, 45) and respond to HBV infection (11). In the same vein, cGAMP has been shown to be packaged in viral particles (46). It would be of interest to determine whether HBV particles can incorporate cGAMP during viral assembly and to test their ability to stimulate other cell types through this indirect pathway.

Moreover, our results show conclusive evidence that cGAS basal expression has antiviral activity against HBV infection including reduction of viral cccDNA. This finding extends a previous studies showing that cGAS exhibited an antiviral activity against a broad range of RNA and DNA viruses (20) and that the cGAS/STING pathway can impair HBV replication and assembly in

transfection studies (24, 25). Schoggins and colleagues have proposed that the expression of cGAS may be responsible for the establishment of a basal antiviral level in the cells through its activation by an unknown ligand. cGAS-depleted cells may then be more susceptible to viral infections through the downregulation of the basal level of innate antiviral genes (20).

Given its antiviral function, cGAS is a target of choice for viruses in order to evade immune responses. It has been reported that the Kaposi's sarcoma-associated herpesvirus negatively regulated cGAS-dependent signaling pathway (47, 48). In the same vein, HBV viral proteins have been shown to interfere with the JAK-STAT signaling pathway (16). Our data suggest that HBV can repress the expression of the cGAS and its related genes, such as *MB21D1*, *TMEM17* and *TBK1*. More interestingly, *MB21D1* expression was downregulated in the liver of HBV-infected mice, validating the relevance of these findings *in vivo*. It still needs to be determined whether HBV can directly target cGAS and cGAS-related factors for an active inhibition of this signaling pathway. A recent study elegantly demonstrated an active inhibition of cGAS pathway by Dengue virus through NS2B protein (49). On the other hand, *MB21D1* (as a classical member of the ISGs (20, 36)) downregulation may be the consequence of the global inhibition of the canonical IFN pathways by HBV as suggested by some investigators (16, 50), but not by others (11, 13, 14). Given the antiviral activity of the cGAS-signaling pathway against HBV including reduction of HBV cccDNA (Figure 5, (24, 25)) the virus-mediated restriction of *MB21D1* expression may play an additional role in HBV immune evasion.

REFERENCES

1. Trepo C, Chan HL, Lok A. Hepatitis B virus infection. Lancet 2014;384:2053-2063.

2. **Zeisel MB, Lucifora J**, Mason WS, Sureau C, Beck J, Levrero M, Kann M, et al. Towards

427 an HBV cure: state-of-the-art and unresolved questions-report of the ANRS workshop on HBV
428 cure. Gut 2015;64:1314-1326.
429 3. Levrero M, Testoni B, Zoulim F. HBV cure: why, how, when? Curr Opin Virol 2016;18:135-
430 143.
431 4. Verrier ER, Colpitts CC, Sureau C, Baumert TF. Hepatitis B virus receptors and molecular
432 drug targets. Hepatol Int 2016;10:567-573.
433 5. Nassal M. Hepatitis B virus cccDNA - viral persistence reservoir and key obstacle for a
434 cure of chronic hepatitis B. Gut 2015;64:1972-1984.
435 6. Lu HL, Liao F. Melanoma differentiation-associated gene 5 senses hepatitis B virus and
436 activates innate immune signaling to suppress virus replication. J Immunol 2013;191:3264-3276.
437 7. **Sato S, Li K, Kameyama T, Hayashi T**, Ishida Y, Murakami S, Watanabe T, et al. The
438 RNA sensor RIG-I dually functions as an innate sensor and direct antiviral factor for hepatitis B
439 virus. Immunity 2015;42:123-132.
440 8. Wieland S, Thimme R, Purcell RH, Chisari FV. Genomic analysis of the host response to
441 hepatitis B virus infection. Proc Natl Acad Sci U S A 2004;101:6669-6674.
442 9. Wieland SF, Chisari FV. Stealth and cunning: hepatitis B and hepatitis C viruses. J Virol
443 2005;79:9369-9380.
444 10. Fletcher SP, Chin DJ, Ji Y, Iniguez AL, Taillon B, Swinney DC, Ravindran P, et al.
445 Transcriptomic analysis of the woodchuck model of chronic hepatitis B. Hepatology 2012;56:820-
446 830.
447 11. Cheng X, Xia Y, Serti E, Block PD, Chung M, Chayama K, Rehermann B, et al. Hepatitis
448 B virus evades innate immunity of hepatocytes but activates macrophages during infection.
449 Hepatology 2017;66:1779-1793.
450 12. **Luangsay S, Gruffaz M**, Isorce N, Testoni B, Michelet M, Faure-Dupuy S, Maadadi S, et

al. Early inhibition of hepatocyte innate responses by hepatitis B virus. J Hepatol 2015;63:1314-1322.

13. Suslov A, Boldanova T, Wang X, Wieland S, Heim MH. Hepatitis B Virus Does Not Interfere with Innate Immune Responses in the Human Liver. Gastroenterology 2018. In press.

14. Mutz P, Metz P, Lempp FA, Bender S, Qu B, Schoneweis K, Seitz S, et al. HBV Bypasses the Innate Immune Response and Does not Protect HCV From Antiviral Activity of Interferon. Gastroenterology 2018. In press.

15. Ferrari C. HBV and the immune response. Liver Int 2015;35 Suppl 1:121-128.

16. Bertoletti A, Ferrari C. Innate and adaptive immune responses in chronic hepatitis B virus infections: towards restoration of immune control of viral infection. Gut 2012;61:1754-1764.

17. Chan YK, Gack MU. Viral evasion of intracellular DNA and RNA sensing. Nat Rev Microbiol 2016;14:360-373.

18. Gao D, Wu J, Wu YT, Du F, Aroh C, Yan N, Sun L, et al. Cyclic GMP-AMP synthase is an innate immune sensor of HIV and other retroviruses. Science 2013;341:903-906.

19. **Sun L, Wu J**, Du F, Chen X, Chen ZJ. Cyclic GMP-AMP synthase is a cytosolic DNA sensor that activates the type I interferon pathway. Science 2013;339:786-791.

20. Schoggins JW, MacDuff DA, Imanaka N, Gainey MD, Shrestha B, Eitson JL, Mar KB, et al. Pan-viral specificity of IFN-induced genes reveals new roles for cGAS in innate immunity. Nature 2014;505:691-695.

21. Xiao TS, Fitzgerald KA. The cGAS-STING pathway for DNA sensing. Mol Cell 2013;51:135-139.

22. **Zhang X, Shi H**, Wu J, Sun L, Chen C, Chen ZJ. Cyclic GMP-AMP containing mixed phosphodiester linkages is an endogenous high-affinity ligand for STING. Mol Cell 2013;51:226-235.

23. **Wu J, Sun L**, Chen X, Du F, Shi H, Chen C, Chen ZJ. Cyclic GMP-AMP is an endogenous second messenger in innate immune signaling by cytosolic DNA. Science 2013;339:826-830.

24. He J, Hao R, Liu D, Liu X, Wu S, Guo S, Wang Y, et al. Inhibition of hepatitis B virus replication by activation of the cGAS-STING pathway. J Gen Virol 2016;97:3368-3378.

25. Dansako H, Ueda Y, Okumura N, Satoh S, Sugiyama M, Mizokami M, Ikeda M, et al. The cyclic GMP-AMP synthetase-STING signaling pathway is required for both the innate immune response against HBV and the suppression of HBV assembly. FEBS J 2016;283:144-156.

26. Verrier ER, Colpitts CC, Schuster C, Zeisel MB, Baumert TF. Cell Culture Models for the Investigation of Hepatitis B and D Virus Infection. Viruses 2016;8.

27. Israelow B, Narbus CM, Sourisseau M, Evans MJ. HepG2 cells mount an effective antiviral interferon-lambda based innate immune response to hepatitis C virus infection. Hepatology 2014;60:1170-1179.

28. Mailly L, Xiao F, Lupberger J, Wilson GK, Aubert P, Duong FH, Calabrese D, et al. Clearance of persistent hepatitis C virus infection in humanized mice using a claudin-1-targeting monoclonal antibody. Nat Biotechnol 2015;33:549-554.

29. **Lupberger J, Zeisel MB**, Xiao F, Thumann C, Fofana I, Zona L, Davis C, et al. EGFR and EphA2 are host factors for hepatitis C virus entry and possible targets for antiviral therapy. Nat Med 2011;17:589-595.

30. Verrier ER, Colpitts CC, Bach C, Heydmann L, Weiss A, Renaud M, Durand SC, et al. A targeted functional RNAi screen uncovers Glypican 5 as an entry factor for hepatitis B and D viruses. Hepatology 2016;63:35–48.

31. **Sanjana NE, Shalem O**, Zhang F. Improved vectors and genome-wide libraries for CRISPR screening. Nat Methods 2014;11:783-784.

32. Lucifora J, Salvetti A, Marniquet X, Mailly L, Testoni B, Fusil F, Inchauspe A, et al.

499 Detection of the hepatitis B virus (HBV) covalently-closed-circular DNA (cccDNA) in mice
500 transduced with a recombinant AAV-HBV vector. Antiviral Res 2017;145:14-19.
501 33. Gao W, Hu J. Formation of hepatitis B virus covalently closed circular DNA: removal of
502 genome-linked protein. J Virol 2007;81:6164-6174.
503 34. Subramanian A, Tamayo P, Mootha VK, Mukherjee S, Ebert BL, Gillette MA, Paulovich A,
504 et al. Gene set enrichment analysis: a knowledge-based approach for interpreting genome-wide
505 expression profiles. Proc Natl Acad Sci U S A 2005;102:15545-15550.
506 35. Wieland S, Makowska Z, Campana B, Calabrese D, Dill MT, Chung J, Chisari FV, et al.
507 Simultaneous detection of hepatitis C virus and interferon stimulated gene expression in infected
508 human liver. Hepatology 2014;59:2121-2130.
509 36. Schoggins JW, Wilson SJ, Panis M, Murphy MY, Jones CT, Bieniasz P, Rice CM. A diverse
510 range of gene products are effectors of the type I interferon antiviral response. Nature
511 2011;472:481-485.
512 37. Blondot ML, Bruss V, Kann M. Intracellular transport and egress of hepatitis B virus. J
513 Hepatol 2016;64:S49-59.
514 38. Cui X, Clark DN, Liu K, Xu XD, Guo JT, Hu J. Viral DNA-Dependent Induction of Innate
515 Immune Response to Hepatitis B Virus in Immortalized Mouse Hepatocytes. J Virol 2015;90:486-
516 496.
517 39. Cui X, Luckenbaugh L, Bruss V, Hu J. Alteration of Mature Nucleocapsid and
518 Enhancement of Covalently Closed Circular DNA Formation by Hepatitis B Virus Core Mutants
519 Defective in Complete-Virion Formation. J Virol 2015;89:10064-10072.
520 40. **Lahaye X, Satoh T**, Gentili M, Cerboni S, Conrad C, Hurbain I, El Marjou A, et al. The
521 capsids of HIV-1 and HIV-2 determine immune detection of the viral cDNA by the innate sensor
522 cGAS in dendritic cells. Immunity 2013;39:1132-1142.

523 41. Thomsen MK, Nandakumar R, Stadler D, Malo A, Valls RM, Wang F, Reinert LS, et al.
524 Lack of immunological DNA sensing in hepatocytes facilitates hepatitis B virus infection.
525 Hepatology 2016;64:746-759.
526 42. **Cho CS, Park HW**, Ho A, Semple IA, Kim B, Jang I, Park H, et al. Lipotoxicity induces
527 hepatic protein inclusions through TBK1-mediated p62/SQSTM1 phosphorylation. Hepatology
528 2017. In press.
529 43. Yang H, Wang H, Ren J, Chen Q, Chen ZJ. cGAS is essential for cellular senescence.
530 Proc Natl Acad Sci U S A 2017;114:E4612-E4620.
531 44. Lei Z, Deng M, Yi Z, Sun Q, Shapiro RA, Xu H, Li T, et al. cGAS-mediated autophagy
532 protects the liver from ischemia/reperfusion injury independent of STING. Am J Physiol
533 Gastrointest Liver Physiol 2018. In press.
534 45. Leong CR, Oshiumi H, Okamoto M, Azuma M, Takaki H, Matsumoto M, Chayama K, et
535 al. A MAVS/TICAM-1-independent interferon-inducing pathway contributes to regulation of
536 hepatitis B virus replication in the mouse hydrodynamic injection model. J Innate Immun
537 2015;7:47-58.
538 46. Gentili M, Kowal J, Tkach M, Satoh T, Lahaye X, Conrad C, Boyron M, et al. Transmission
539 of innate immune signaling by packaging of cGAMP in viral particles. Science 2015;349:1232-
540 1236.
541 47. **Wu JJ, Li W**, Shao Y, Avey D, Fu B, Gillen J, Hand T, et al. Inhibition of cGAS DNA
542 Sensing by a Herpesvirus Virion Protein. Cell Host Microbe 2015;18:333-344.
543 48. Li W, Avey D, Fu B, Wu JJ, Ma S, Liu X, Zhu F. Kaposi's Sarcoma-Associated Herpesvirus
544 Inhibitor of cGAS (KicGAS), Encoded by ORF52, Is an Abundant Tegument Protein and Is
545 Required for Production of Infectious Progeny Viruses. J Virol 2016;90:5329-5342.
546 49. Aguirre S, Luthra P, Sanchez-Aparicio MT, Maestre AM, Patel J, Lamothe F, Fredericks

AC, et al. Dengue virus NS2B protein targets cGAS for degradation and prevents mitochondrial DNA sensing during infection. Nat Microbiol 2017;2:17037.

50. Ortega-Prieto AM, Skelton JK, Wai SN, Large E, Lussignol M, Vizcay-Barrena G, Hughes D, et al. 3D microfluidic liver cultures as a physiological preclinical tool for hepatitis B virus infection. Nat Commun 2018;9:682.

Author names in bold designate shared co-first authorship.

Acknowledgments: We thank D. Garcin (University of Geneva, Switzerland) for providing the SeV inoculum; D. Calabrese, S. Wieland and M. Heim (University of Basel, Switzerland) for the FISH analyses and helpful discussions; F. Zhang (Broad Institute of MIT and Harvard, Cambridge, MA, USA) for lentiCas9-Blast and lentiGuide-Puro plasmids, C. Thumann, N. Brignon, and M. Oudot (Inserm U1110) for excellent technical support, and J.M. Rousée from Laboratoire Schuh-groupement Bio 67 (Strasbourg) for the quantification of HBV loads in sera of humanized mice.

Conflict of interest: The authors declare no competing financial interests.

Author contribution. TFB initiated the study. TFB, ERV and CS designed and supervised research. ERV, SAY, LH, CB, VTL, SD, LM, JL, TC and DD performed the experiments. ERV, SAY, LH, CB, VTL, JL, DD, MBZ, NP, CS and TFB analyzed the data. PP provided liver resections for PHH isolation. NM, IH and NP made substantive intellectual contributions. ERV, SAY, CS and TFB wrote the paper.

FIGURE LEGENDS

Figure 1. cGAS expression and function in human hepatocytes and in a cell culture model for HBV infection. (A) Detection of endogenous cGAS protein expression in different cellular models by Western blot. Cell lysates from Huh7.5.1, HepG2, HepG2-NTCP cells, and PHH from three independent donors were used. HepG2-NTCP cells were reverse transfected with a siRNA targeting *MB21D1* (sicGAS) or a non-targeting siRNA control (siCtrl) two days before cGAS detection. β-actin was used as a Western blot control. Individual representative experiments are shown. (B) Generation of *MB21D1* knock out (KO) cells. *MB21D1* KO HepG2-NTCP cell lines were generated via CRISPR/Cas9 technology. The absence or presence of cGAS protein was controlled by Western blot using the HPA031700 anti-cGAS antibody in Cas9-expressing HepG2-NTCP cells (Cas9) and in different cell lines after transduction with the sgRNA targeting *MB21D1* (line-A, line-B, line-C, cGAS_KO#1 and cGAS_KO#2). One experiment is shown. (C) Detection of endogenous STING protein in HepG2-NTCP cells. siRNA targeting *TMEM173* (siSTING) or a non-targeting siRNA (siCtrl) were reverse-transfected into HepG2-NTCP cells. Silencing efficacy was assessed by Western blot. One experiment is shown. (D-E) Poly (I:C) and dsDNA transfection induce *IFNB1* and *MB21D1* expression in HepG2-NTCP cells. HepG2-NTCP cells were transfected with increasing doses of Poly (I:C) or calf thymus DNA at the indicated concentrations. *IFNB1* mRNA expression was quantified by qRT-PCR 24 h after transfection and cGAS protein expression was assessed by Western blot 24 h and 48 h after transfection. qRT-PCR data (D) are expressed as means ± SD relative *IFNB1* expression (log10) compared to non-transfected control (0, set at 100) from four independent experiments performed in triplicate (dsDNA) or from three independent experiments performed in triplicate (Poly I:C). One representative Western blot experiment is shown (E).

Figure 2. Impaired cGAS-mediated sensing of HBV infection in HepG2-NTCP cells. (A-B) HBV infection does not induce *IFNB1* or *IFNL1* expression. HepG2-NTCP cells were infected with HBV (MOI: 500) or SeV (MOI: 10) and total RNA was extracted every day for 3 days. RNA extracted from naive cells before infection was used as a control (D0). *IFNB1* (A) and *IFNL1* (B) expression was then assessed by qRT-PCR. Results are expressed as means ± SD *IFNB1/IFNL1* relative expression (log10) compared to controls (D0, all set at 1) from three independent experiments performed at least in duplicate (SeV) or four independent experiments performed in duplicate (HBV). No robust *IFNL1* expression was detected in HBV-infected samples (representative dots are presented under the “detection limit” dotted line). (C, E) cGAS-related ISGs are not affected by HBV infection. HepG2-NTCP cells were infected with HBV or SeV. Alternatively, HepG2-NTCP cells were transfected with Poly (I:C) (100ng). Two days after infection or transfection, total RNA was extracted. Gene expression of IAR signature was then analyzed using multiplexed gene profiling. Results were analyzed by GSEA enrichment compared to non-transfected or non-infected controls (C) or by *IFNB1* and *IFI44* gene expression (log10) compared to non-transfected or non-infected controls (set at 1) (E). One experiment performed in triplicate is shown. (D, F) cGAS expression level does not affect the cellular response to HBV infection. HepG2-NTCP-Cas9 (Cas9), HepG2-NTCP-KO_cGAS#2 (Ko_cGAS#2), HepG2-NTCP-Ctrl_ORF (Ctrl_ORF), and HepG2-NTCP-cGAS_OE (cGAS_OE) were infected with HBV. Two days after infection, total RNA was extracted. Gene expression of IAR signature gene set was then analyzed using multiplexed gene profiling. Results were analyzed by GSEA enrichment compared to non-transfected or non-infected controls (D) or by *IFNB1* and *IFI44* gene expression (log10) compared to non-transfected or non-infected controls (set at 1) (F). One experiment performed in triplicate is shown. IAR: innate antiviral response gene set.

Figure 3. Impaired sensing of HBV infection at high MOIs or early time points of infection. (A-C) HepG2-NTCP cells were infected with HBV at increasing MOIs (0, 50, 500, and 10000 GEq/cell) or transfected with Poly (I:C) (100 ng). Two days after infection or transfection, cells were lysed, total RNA was extracted, and *IFNB1* expression (A) as well as HBV pgRNA levels (B) were quantified by qRT-PCR. (A) Results are expressed as means ± SD relative *IFNB1* expression (log10) compared to mock infected cells (MOI 0, set at 1) from three independent experiments performed in triplicate. (B) Results are expressed means ± SD relative HBV pgRNA levels compared to mock infected cells (MOI 0, set at 100%) from three independent experiments performed in triplicate. Alternatively, HBV infection was assessed at 10 days post infection by IF of HBsAg (C). One representative experiment is shown. (D) HBV infection does not induce *IFNB1* expression at early time points. HepG2-NTCP cells were either infected by HBV or SeV, or transfected with Poly (I:C). Total RNA was extracted at 2 h, 6 h, 18 h, and 24 h post infection/transfection and *IFNB1* expression was assessed by qPCR. Results are expressed as means ± SD relative *IFNB1* expression (log10) compared to naive cells (0, set at 1) from three independent experiments performed in triplicate.

Figure 4. Sensing of HBV rcDNA in HepG2-NTCP cells. (A-B) Transfection of purified HBV rcDNA genome induces a cGAS-mediated innate immune response. HBV rcDNA was extracted from recombinant HBV virions as described in Experimental Procedures and quantified by qPCR (Figure S3). HBV rcDNA (1 µg) and positive control dsDNA (1 µg) were transfected into HepG2-NTCP-Cas9 and HepG2-NTCP-KO_cGAS#2 cells. Three days after transfection, total RNA was extracted. Gene expression of IAR set was then analyzed using multiplexed gene profiling. The transcripts were analyzed by GSEA enrichment compared to non-transfected control (A) or by

IFNB1 and *IFI44* gene expression (log10) compared to non-transfected control (set at 1) (B). One experiment in triplicate is shown. (C) HBV DNA in HepG2-NTCP cells after rcDNA transfection and HBV infection are similar. HepG2-NTCP were infected with HBV or transfected with HBV rcDNA (1µg). At day 2 after transfection/infection, DNA was extracted and total HBV DNA was quantified by qPCR. Results are expressed as means ± SD total DNA copies per µg of total DNA (log10) from three independent experiments performed in triplicate (HBV infection) and two independent experiments performed in triplicate (HBV rcDNA transfection). IAR: innate antiviral response gene set.

Figure 5. Sensing of naked HBV rcDNA but not infectious HBV virions in primary human hepatocytes. (A-B) HBV infection does not induce ISG expression in PHH. PHH were treated with a preS1 peptide (PreS1) or a scrambled peptide (Ctrl) for one hour before infection with HBV. As positive controls, PHH were transfected with Poly (I:C) (100ng) or infected with SeV (MOI ~ 10). HBV infection of PHH was assessed 10 days post infection by qRT-PCR (A, left panel) or immunofluorescence (A, right panel). qRT-PCR results are expressed as means ± SD ratio HBV pgRNA RNA / GAPDH mRNA from one experiment corresponding to the gene profiling experiment and performed in duplicate. Two days after infection, total RNA was extracted and gene expression of IAR was then analyzed using multiplexed gene profiling. Results were analyzed by GSEA enrichment compared to non-transfected control (B). One experiment in triplicate is shown. (C) Induction of *IFBN1* and *IFNL1* expression in PHH. PHH were transfected with dsDNA (4 µg) or HBV rcDNA (4 µg). *IFNB1*- and *IFNL1* expression was assessed 24 h after transfection by qRT-PCR. Results are expressed as means ± SD log10 *IFNB1* or *IFNL1* expression compared to non-transfected control cells (Ctrl, set at 1) from five independent experiments performed at least in duplicate. IAR: innate antiviral response gene set.

Figure 6. Antiviral activity of cGAS results in reduction of HBV cccDNA. (A-B) Silencing of cGAS-related gene expression increases HBV infection. siRNA targeting *MB21D1* (sicGAS), *TMEM173* (siSTING), *TBK1* (siTBK1), *IFI16* (siIFI16) or a non-targeting siRNA (siCtrl) were reverse-transfected into HepG2-NTCP cells 2 days prior to HBV infection. Silencing efficacy was assessed by qRT-PCR 2 days after transfection (A). Results are expressed as means ± SD % gene expression relative to siCtrl (set at 100%) from four independent experiments performed in technical duplicate. HBV infection was assessed by quantification of HBV pgRNA by qRT-PCR 10 days after infection (B). Results are expressed as means ± SD % HBV pgRNA expression relative to siCtrl (set at 100%) from four independent experiments performed in technical duplicate. (C) KO of *MB21D1* gene increases HBV infection. cGAS_KO#1, cGAS_KO#2, and the control Cas9 cells were then infected with HBV and viral infection was assessed 10 days after infection as described above. Results are expressed as means ± SD % HBV pgRNA expression relative to control cell line (Cas9, set at 100%) from three independent experiments performed in triplicate. (D) cGAS overexpression reduces HBV infection. HepG2-NTCP cells were transduced with lentivirus encoding either a control plasmid (Ctrl_ORF) or a plasmid encoding the full length *MB21D1* ORF (cGAS_OE). *MB21D1* expression was assessed by qRT-PCR (left panel). Results are expressed as means ± SD % relative *MB21D1* expression (log10) relative to control cell line (Ctrl_ORF, set at 1) from three independent experiments performed in duplicate. HepG2-NTCP, Ctrl_ORF, and cGAS_OE cells were then infected with HBV for ten days and HBV infection was assessed as described above. Results are expressed as means ± SD % HBV pgRNA expression relative to control cell line (Ctrl_ORF, set at 100%) from three independent experiments performed in triplicate. (E) Detection of HBV cccDNA by Southern blot. HepG2-NTCP-derived cGAS_KO- or

689 cGAS_overexpressing cell lines were infected for 10 days with HBV. Total DNA from indicated
690 HBV infected cells was extracted and HBV DNA were detected by Southern blot. Two different
691 DNA ladders (L1 & L2) were used. *XhoI* digestion of DNA extracted from HBV-infected HepG2-
692 NTCP-Cas9 cells was used as a control and resulted in a single 3.2 kb band (dsl HBV DNA).
693 Mitochondrial DNA (mt DNA) was detected as a loading control. One experiment is shown.
694
695 **Figure 7. HBV infection suppresses the expression of the cGAS-related genes cell culture**
696 **and humanized liver chimeric mice *in vivo*.** (A-C) HepG2-NTCP cells were infected with HBV
697 for 10 days. HBV infection was assessed by quantification of HBV pgRNA by qRT-PCR. Results
698 are expressed as means ± SD from three experiments performed in triplicate. cGAS protein
699 expression was assessed 10 days after infection (B, one experiment is shown). Gene expression
700 relative to non-infected control cells of *MB21D1*, *TMEM173* and *TBK1* were assessed by qRT-
701 PCR at day 10 after infection (C). Results are expressed as means ± SEM from three independent
702 experiments performed in triplicate. (D-E) *MB21D1*- and IAR gene set expression is impaired in
703 HBV-infected mice. uPA-SCID mice were infected with HBV for 16 weeks. Mice were then
704 sacrificed and HBV infection was assessed by HBV RNA specific in situ hybridization (D) and
705 quantification of HBV viral load in the serum (Table 1). Human *MB21D1* expression was detected
706 in human hepatocytes by FISH from one HBV-infected mouse (D) and by qRT-PCR from 7 HBV-
707 infected mice and 4 control mice (E, left panel). Results are expressed as the ratio *MB21D1* mRNA
708 / *GAPDH* mRNA. All individual mice are presented as well as means ± SD for each group (Mock-
709 and HBV-infected mice). The level of *MB21D1* expression was independent of the viability of
710 engrafted human hepatocytes as indicated by an absent correlation between *MB21D1* expression
711 and the human serum albumin expression in humanized mice ($R^2 = 0.231$, E, right panel). (F) The
712 IAR gene set was analyzed using the nCounter NanoString in mice 6472, 6251, and 6254 (Mock-

infected mice, Table 1) and 4766, 4771, and 4847 (HBV-infected mice, Table 1). A significant downregulation (FDR = 0.047) of the gene set was observed in HBV-infected mice compared to control mice. Individual Z-scores for the genes significantly modulated between the two groups according to GSEA analysis are presented. Negative Z-score (blue) and positive Z-score (red) correspond to repression and induction of the indicated genes, respectively. Dpi: days post infection.

Figure 1.

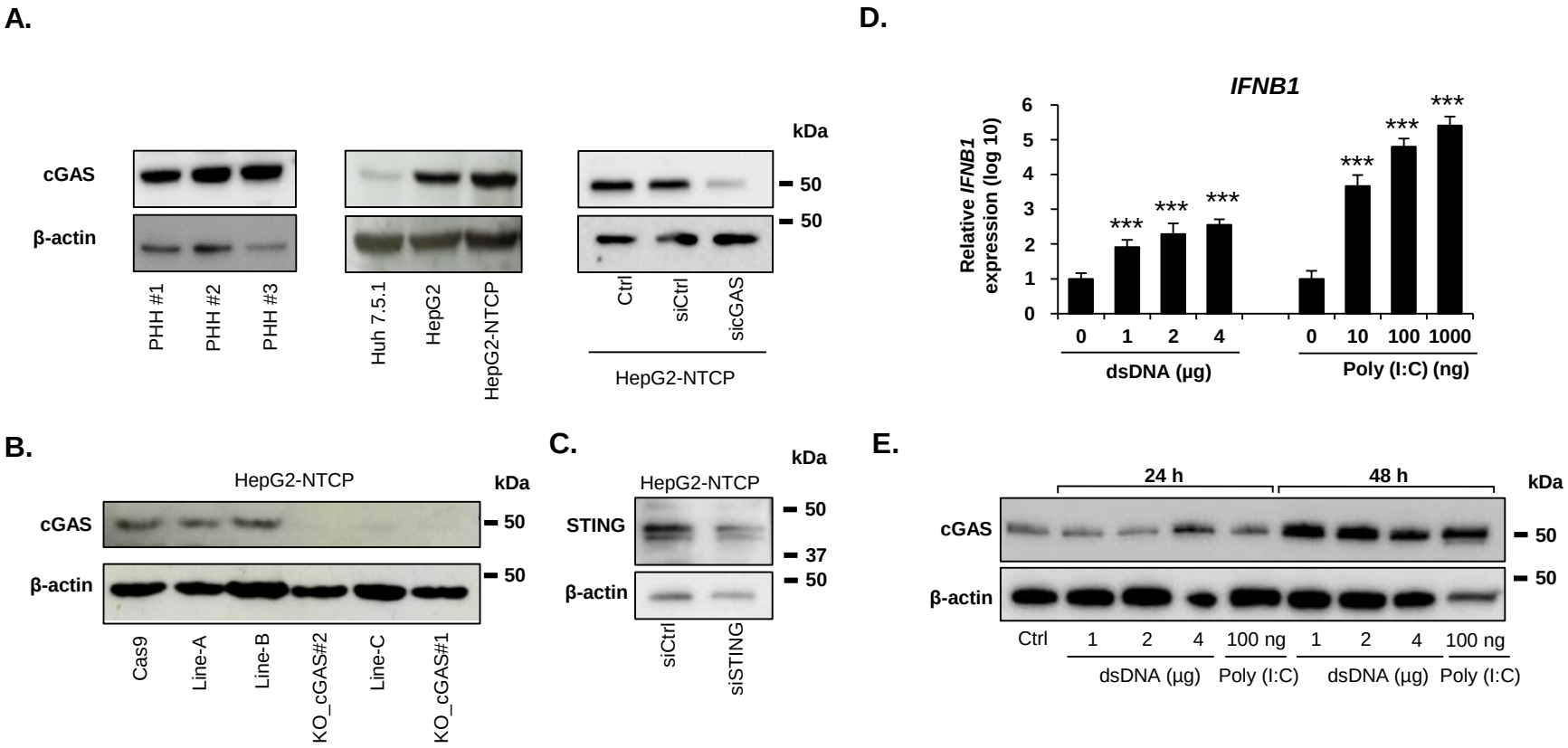
A.
cGAS
β-actin
PHH #1
PHH #2
PHH #3
Huh 7.5.1
HepG2
HepG2-NTCP
kDa
50
50
Ctrl
siCtrl
siCGAS
HepG2-NTCP
B.
HepG2-NTCP
kDa
cGAS
β-actin
50
50
Cas9
Line-A
Line-B
KO_cGAS#2
Line-C
KO_cGAS#1
C.
HepG2-NTCP
kDa
STING
β-actin
50
37
50
siCtrl
siSTING
D.
IFNB1
Relative IFNB1 expression (log 10)
0
1
2
3
4
5
6
***
***
***
***
***
***
0
1
2
4
0
10
100
1000
dsDNA (μg)
Poly (I:C) (ng)
E.
24 h
48 h
kDa
cGAS
β-actin
50
50
Ctrl
1
2
4
100 ng
1
2
4
100 ng
dsDNA (μg)
Poly (I:C)
dsDNA (μg)
Poly (I:C)

Figure 2.

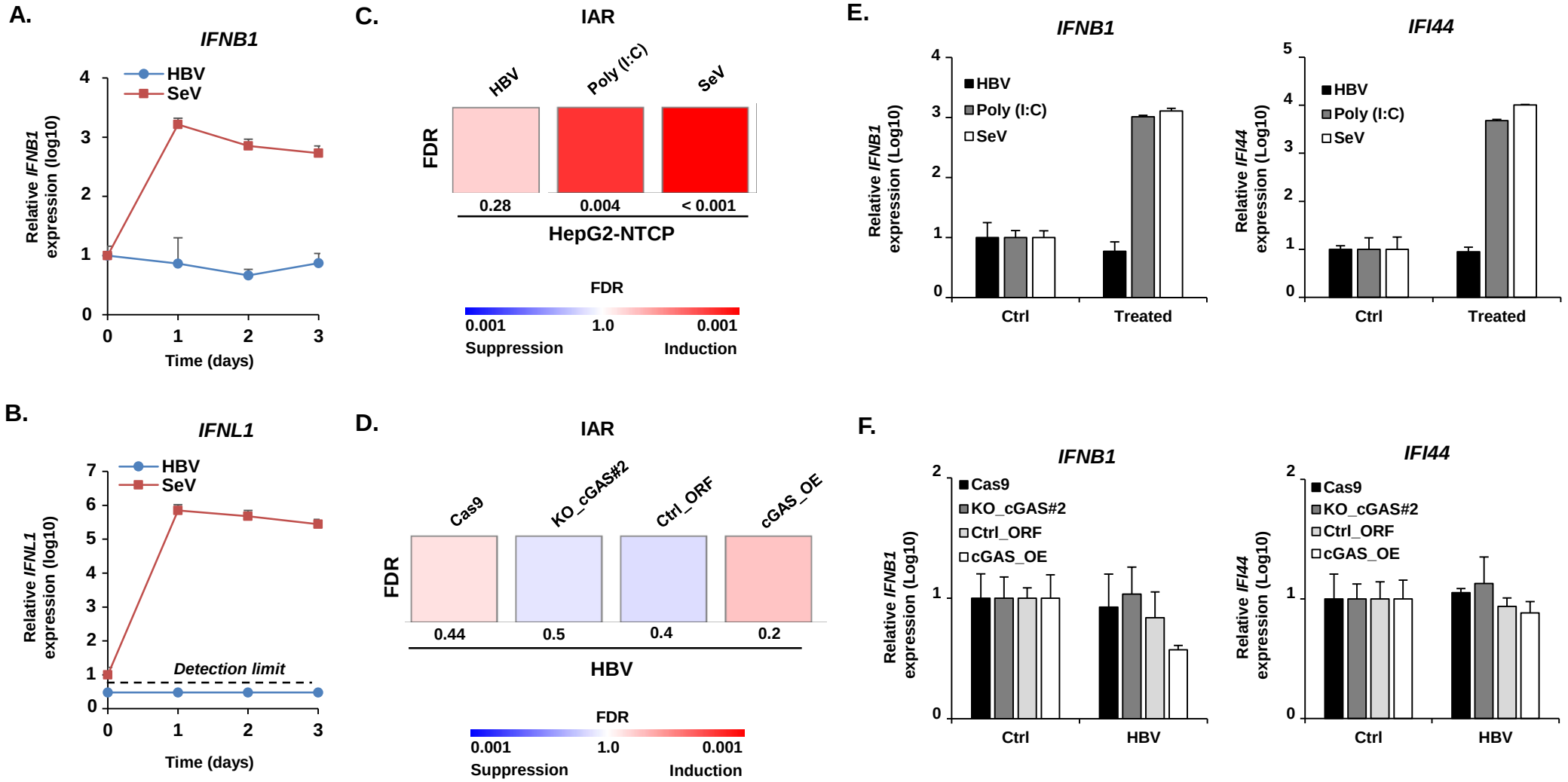
A.
IFNB1
HBV
SeV
Relative IFNB1 expression (log10)
Time (days)
B.
IFNL1
HBV
SeV
Detection limit
Relative IFNL1 expression (log10)
Time (days)
C.
IAR
HBV
Poly (I:C)
SeV
FDR
0.28
0.004
< 0.001
HepG2-NTCP
FDR
0.001
1.0
0.001
Suppression
Induction
D.
IAR
Cas9
KO_cGAS#2
Ctrl_ORF
cGAS_OE
FDR
0.44
0.5
0.4
0.2
HBV
FDR
0.001
1.0
0.001
Suppression
Induction
E.
IFNB1
HBV
Poly (I:C)
SeV
Relative IFNB1 expression (Log10)
Ctrl
Treated
IFI44
HBV
Poly (I:C)
SeV
Relative IFI44 expression (Log10)
Ctrl
Treated
F.
IFNB1
Cas9
KO_cGAS#2
Ctrl_ORF
cGAS_OE
Relative IFNB1 expression (Log10)
Ctrl
HBV
IFI44
Cas9
KO_cGAS#2
Ctrl_ORF
cGAS_OE
Relative IFI44 expression (Log10)
Ctrl
HBV

Figure 3.

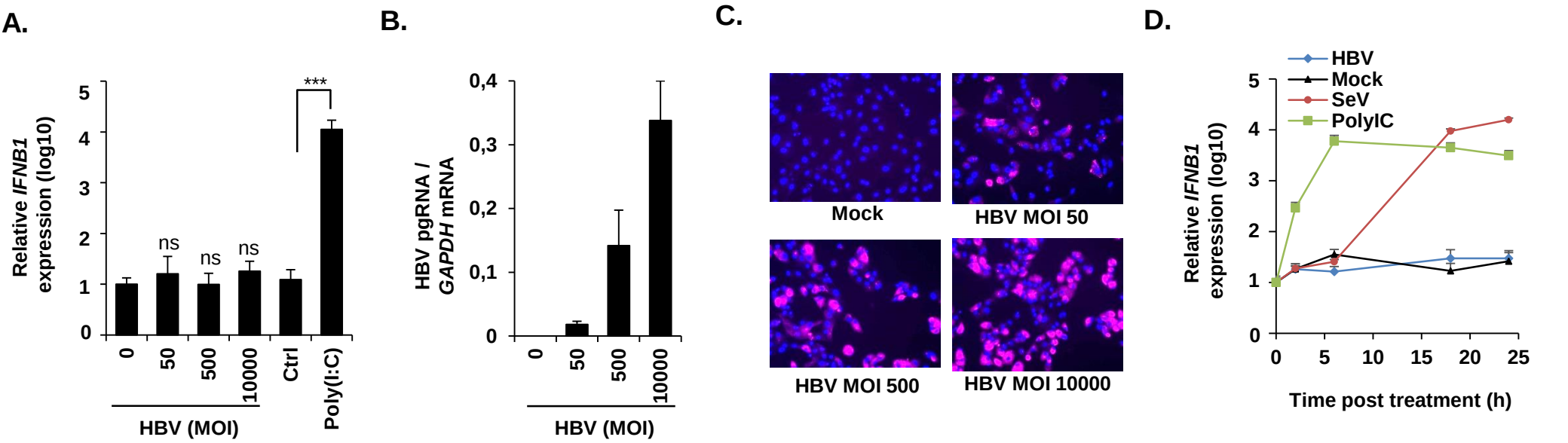
A.
Relative IFNB1 expression (log10)
5
4
3
2
1
0
ns
ns
ns
***
0
50
500
10000
Ctrl
Poly(I:C)
HBV (MOI)
B.
HBV pgRNA / GAPDH mRNA
0,4
0,3
0,2
0,1
0
0
50
500
10000
HBV (MOI)
C.
Mock
HBV MOI 50
HBV MOI 500
HBV MOI 10000
D.
HBV
Mock
SeV
PolyIC
Relative IFNB1 expression (log10)
5
4
3
2
1
0
0
5
10
15
20
25
Time post treatment (h)

Figure 4.

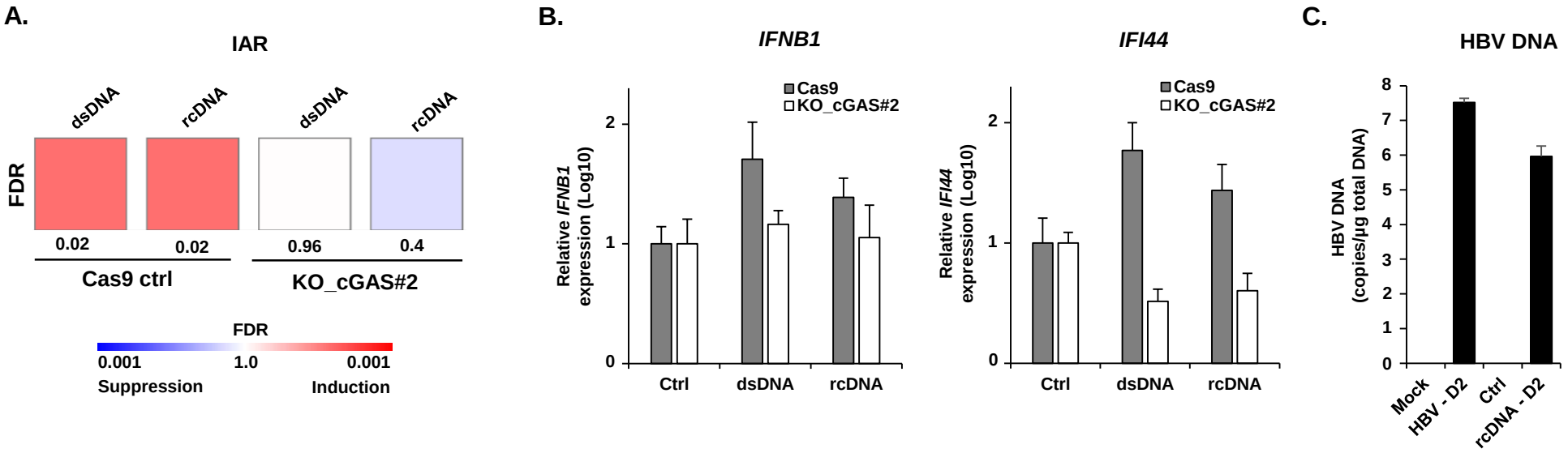
A.
IAR
dsDNA
rcDNA
dsDNA
rcDNA
FDR
0.02
0.02
0.96
0.4
Cas9 ctrl
KO_cGAS#2
FDR
0.001
1.0
0.001
Suppression
Induction
B.
IFNB1
Cas9
KO_cGAS#2
Relative IFNB1 expression (Log10)
2
1
0
Ctrl
dsDNA
rcDNA
IFI44
Cas9
KO_cGAS#2
Relative IFI44 expression (Log10)
2
1
0
Ctrl
dsDNA
rcDNA
C.
HBV DNA
HBV DNA (copies/µg total DNA)
8
7
6
5
4
3
2
1
0
Mock
HBV - D2
Ctrl
rcDNA - D2

Figure 5.

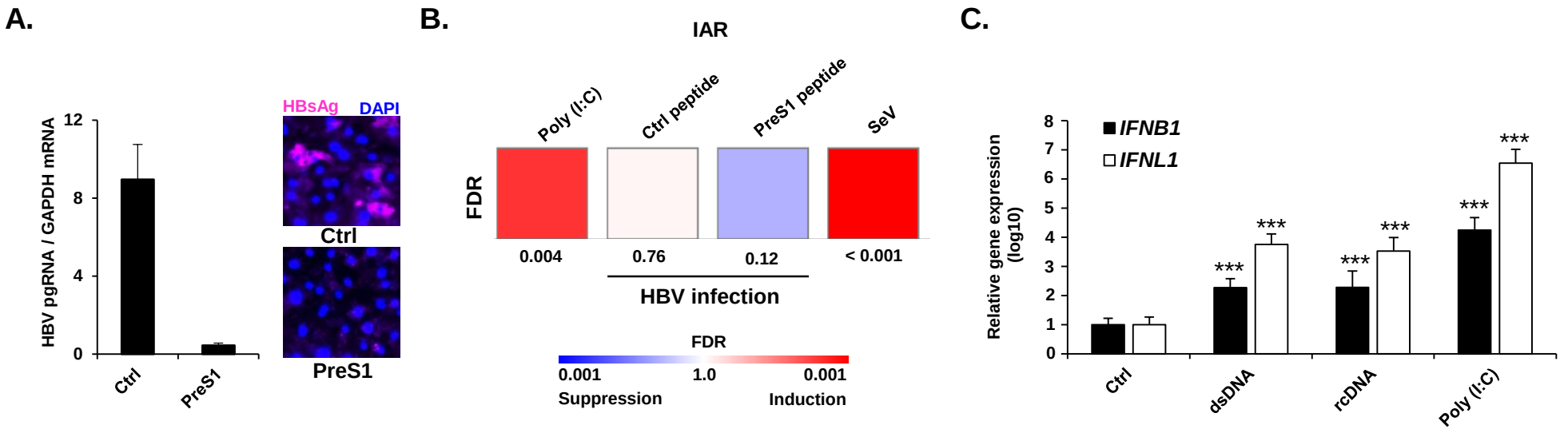
A.
HBV pgRNA / GAPDH mRNA
12
8
4
0
Ctrl
PreS1
HBsAg
DAPI
Ctrl
PreS1
B.
IAR
Poly (I:C)
Ctrl peptide
PreS1 peptide
SeV
FDR
0.004
0.76
0.12
< 0.001
HBV infection
FDR
0.001
1.0
0.001
Suppression
Induction
C.
Relative gene expression (log10)
IFNB1
IFNL1
8
7
6
5
4
3
2
1
0
***
Ctrl
dsDNA
rcDNA
Poly (I:C)

Figure 6.

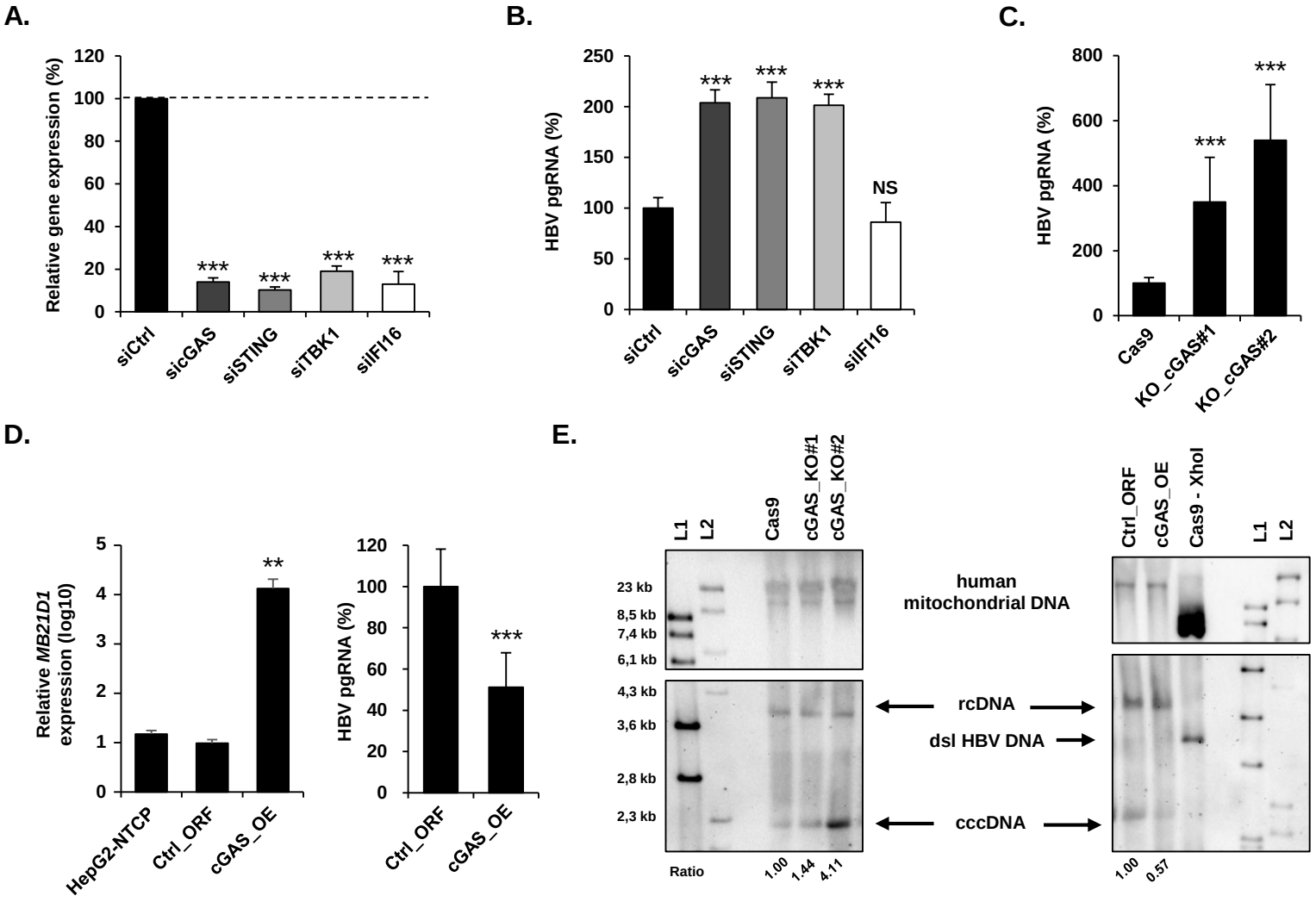
A.
Relative gene expression (%)
120
100
80
60
40
20
0
***
***
***
***
siCtrl
sicGAS
siSTING
siTBK1
siIFI16
B.
HBV pgRNA (%)
250
200
150
100
50
0
***
***
***
NS
siCtrl
sicGAS
siSTING
siTBK1
siIFI16
C.
HBV pgRNA (%)
800
600
400
200
0
***
***
Cas9
KO_cGAS#1
KO_cGAS#2
D.
Relative MB21D1 expression (log10)
5
4
3
2
1
0
**
HepG2-NTCP
Ctrl_ORF
cGAS_OE
HBV pgRNA (%)
120
100
80
60
40
20
0
***
Ctrl_ORF
cGAS_OE
E.
L1
L2
Cas9
cGAS_KO#1
cGAS_KO#2
23 kb
8,5 kb
7,4 kb
6,1 kb
4,3 kb
3,6 kb
2,8 kb
2,3 kb
Ratio
1.00
1.44
4.11
human mitochondrial DNA
rcDNA
dsl HBV DNA
cccDNA
Ctrl_ORF
cGAS_OE
Cas9 - XhoI
L1
L2
1.00
0.57

Figure 7.

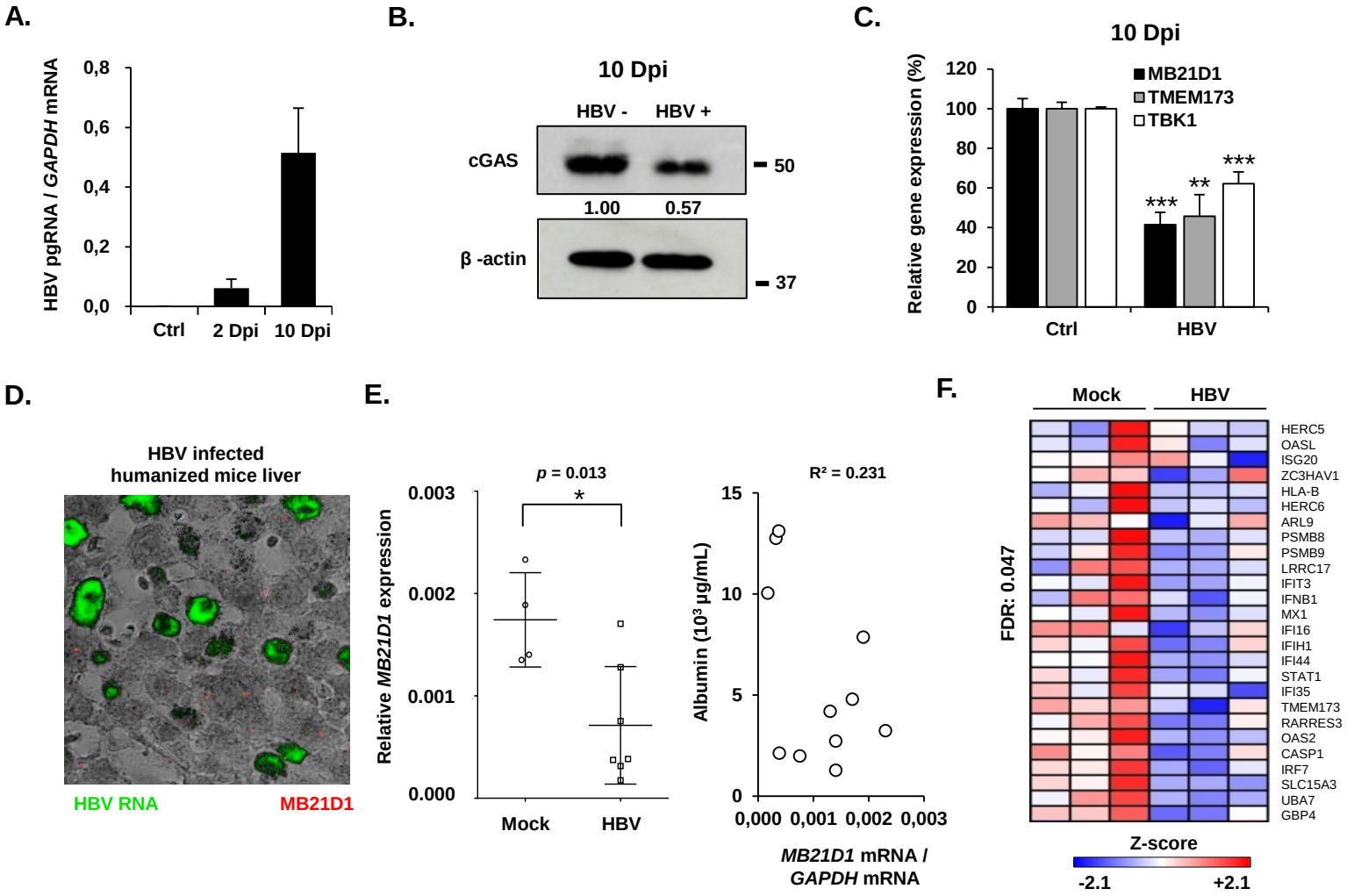
A.
HBV pgRNA / GAPDH mRNA
0,8
0,6
0,4
0,2
0,0
Ctrl
2 Dpi
10 Dpi
B.
10 Dpi
HBV -
HBV +
cGAS
50
1.00
0.57
β -actin
37
C.
10 Dpi
Relative gene expression (%)
120
100
80
60
40
20
0
MB21D1
TMEM173
TBK1
***
**
***
Ctrl
HBV
D.
HBV infected humanized mice liver
HBV RNA
MB21D1
E.
p = 0.013
*
Relative MB21D1 expression
0.003
0.002
0.001
0.000
Mock
HBV
R² = 0.231
Albumin (10³ µg/mL)
15
10
5
0
0,000 0,001 0,002 0,003
MB21D1 mRNA / GAPDH mRNA
F.
Mock
HBV
FDR: 0.047
HERC5
OASL
ISG20
ZC3HAV1
HLA-B
HERC6
ARL9
PSMB8
PSMB9
LRRC17
IFIT3
IFNB1
MX1
IFI16
IFIH1
IFI44
STAT1
IFI35
TMEM173
RARRES3
OAS2
CASP1
IRF7
SLC15A3
UBA7
GBP4
Z-score
-2.1
+2.1

Hepatitis B virus evasion from cGAS sensing in human hepatocytes

Eloi R. Verrier, Seung-Ae Yim, Laura Heydmann, Houssein El Saghire, Laurent Mailly, Charlotte Bach, Vincent Turon-Lagot, Sarah C. Durand, Julie Lucifora, David Durantel, Patrick Pessaux, Nicolas Manel, Ivan Hirsch, Mirjam B. Zeisel, Nathalie Pochet, Catherine Schuster and Thomas F. Baumert

SUPPORTING INFORMATION

Supplementary Experimental Procedures

Detection of cGAS protein expression using two independent antibodies. HepG2-NTCP cells were transfected with a siRNA targeting *MB21D1* expression (sicGAS) or with a non-targeting siRNA control (siCtrl). Three days after transfection, cells were lysed and cGAS protein expression was assessed as described in the Experimental Procedures section using two rabbit polyclonal anti-cGAS antibodies (HPA031700, Sigma & NBP1-86761, Novus Biologicals). Given the proximity of the bands, another western blot was run in parallel for the detection of β-actin as a control. Molecular weights were assessed using the Precision Plus Protein™ Standards molecular weight marker (Bio-Rad).

Detection of HBV DNA by PCR and qPCR. DNA was extracted using QiaAMP DNA MiniKit (Qiagen) following manufacturer's instructions. The presence of HBV DNA was confirmed by PCR using the following primers (expected band size: 148 bp) (1) : forward primer 5'-CACCTCGCCTAATCATC-3', reverse primer 5'-GGAAAGAAGTCAGAAGGCA-3'. For qPCR quantification of HBV DNA, The presence of HBV DNA was confirmed by PCR and quantified by qPCR using the following primers and probe (1) : forward primer 5'-CACCTCGCCTAATCATC-3', reverse primer 5'-GGAAAGAAGTCAGAAGGCA-3'; TaqMan probe 5'-[6FAM]-TGGAGGCTTCAACAGTAGGACATGAAC-[BHQ1]-3'. Copy number of HBV was determined using a standard curve.

Detection of NTCP expression by flow cytometry. HepG2 cells, HepG2-NTCP-Ctrl_ORF cells, and HepG2-NTCP-cGAS_OE cells were treated with the AF647-labelled pres1 peptide for one hour at 37°C as described (1). Cells were then fixed with 2% paraformaldehyde for 20 minutes at room temperature. NTCP expression was then quantified by flow cytometry using MacsQuant instrument (Miltenyi).

Supplementary Figures

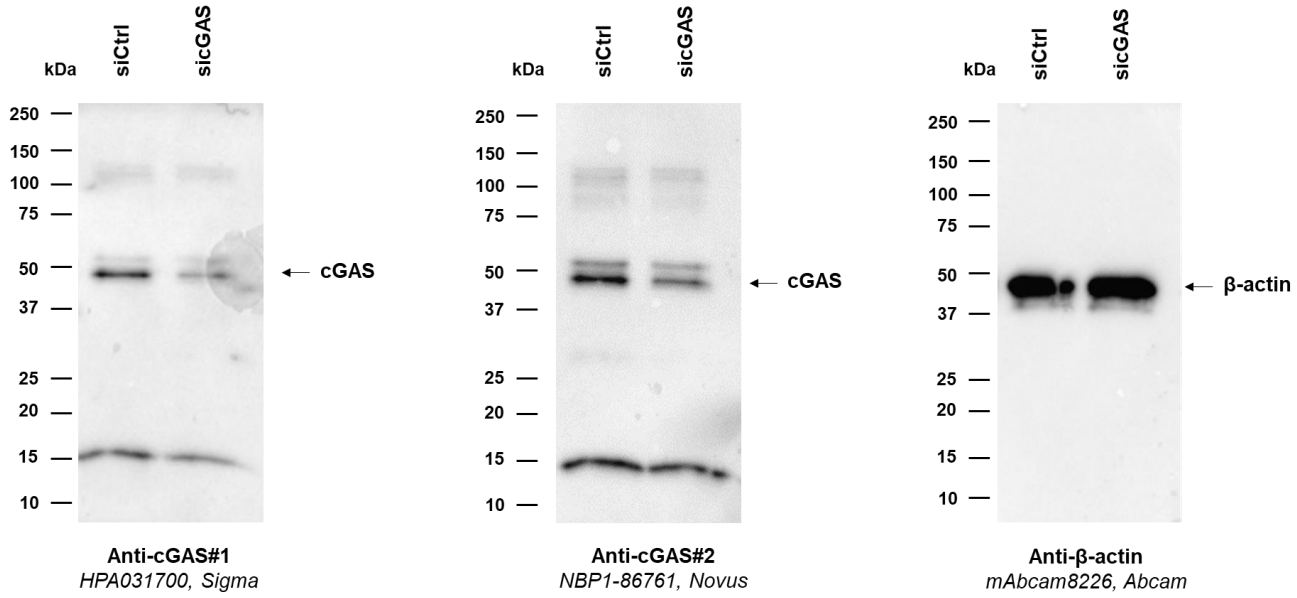

Figure S1. Detection of cGAS protein in HepG2-NTCP cells (related to Figure. 1). HepG2-NTCP cells were transfected for three days with a siRNA targeting *MB21D1* expression (sicGAS) or with a non-targeting siRNA control (siCtrl). Cells were then lysed and cGAS protein expression was assessed using two rabbit polyclonal anti-cGAS antibodies (HPA031700, Sigma, used in the main manuscript & NBP1-86761, Novus Biologicals). β-actin expression was assessed as a control. One representative experiment is shown.

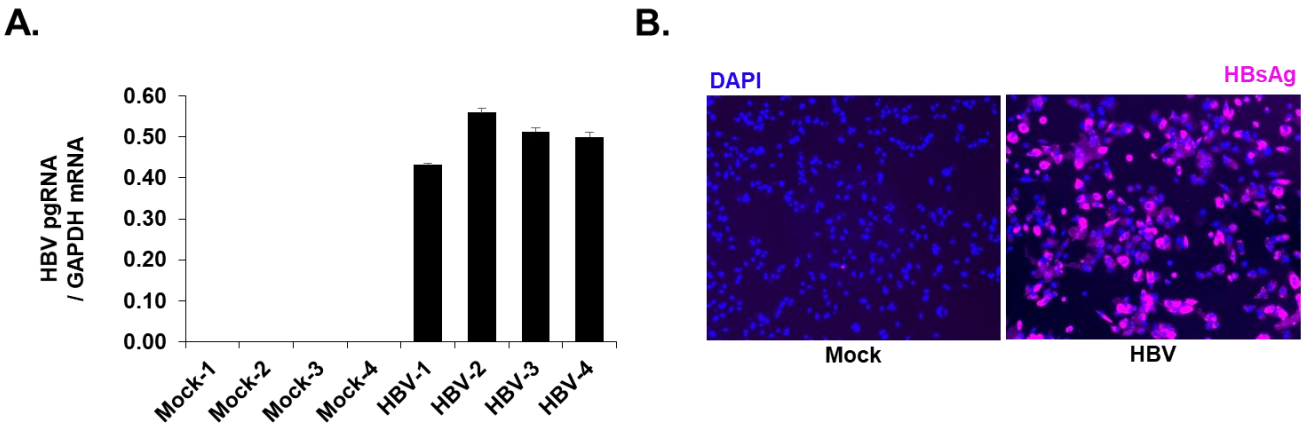

Figure S2. Analysis of HBV infection in HBV time course samples with quantification of HBV pregenomic RNA and HBsAg expression (related to Figure 2). HepG2-NTCP cells were infected with HBV as described in Experimental Procedures. 10 days after infection, total RNA was extracted and HBV infection was assessed by quantification of HBV pgRNA as described in Methods. Results are expressed as means ± SD HBV pgRNA / GAPDH mRNA from four independent experiments performed in duplicate (corresponding to the four experiments shown in Figure 2A). Alternatively, cells were infected for 10 days in HBV, and HBV infection was assessed by immunofluorescence using an anti-HBsAg antibody. One representative experiment is shown.

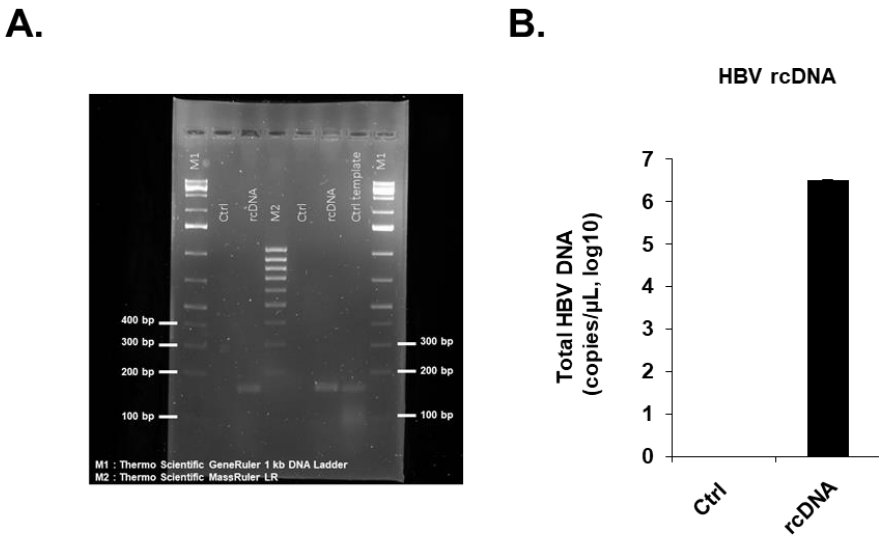

Figure S3. Analysis and quantification of HBV DNA extracted from HBV infectious particles by PCR (related to Figure 4). A-B. HBV genomic DNA (rcDNA) was extracted from cell culture-derived HBV virions. Extraction from naive HepG2-NTCP control supernatants without virus was used as a control (Ctrl). HBV DNA standard preparation used as a template for the calculation of HBV DNA concentration was used as a positive control (Ctrl template). The presence of HBV DNA was controlled by PCR (expected band size: 148 base pairs [bp]) (A) and quantified by qPCR (B). Two independent experiments (A) and one experiment performed in triplicate (B) are shown. C. Quantification of total HBV DNA in transfected or infected cells. HepG2-NTCP were infected with HBV or transfected with rcDNA. Three days after transfection/infection, DNA was extracted and total HBV DNA was quantified by qPCR.

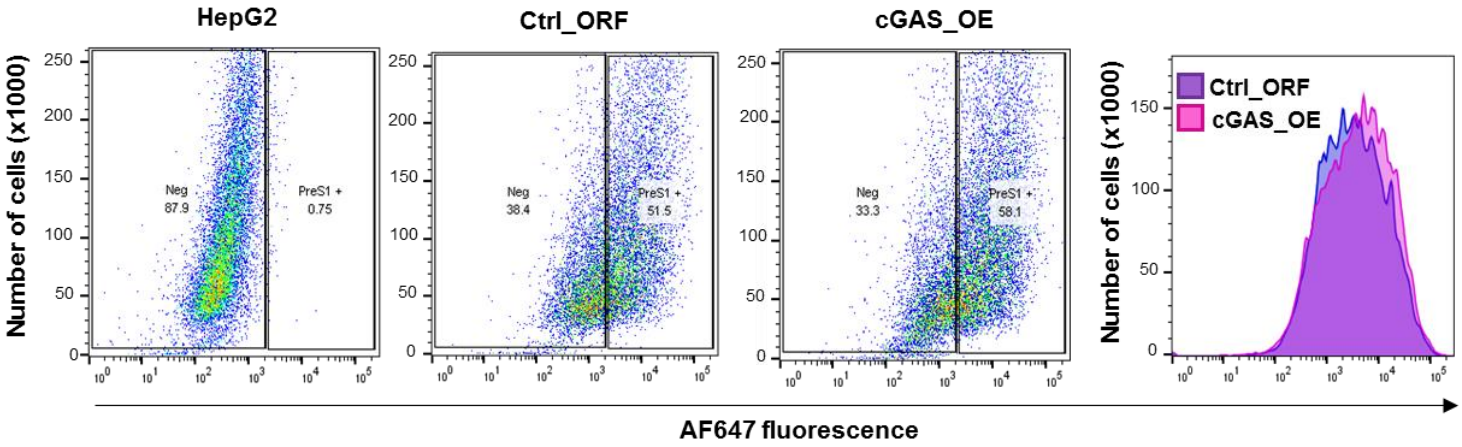

Figure S4. PreS1-binding/NTCP cell surface expression is independent on cGAS expression. HepG2 cells, HepG2-NTCP-Ctrl_ORF cells, and HepG2-NTCP-cGAS_OE cells were treated with the AF647-labelled preS1 peptide for one hour at 37°C. PreS1 binding corresponding to NTCP expression was quantified by flow cytometry.

Supplementary Tables

Tables S1: Specific probes used for the detection of HBV and Mitochondrial DNA (2).

Target	Name	Sequence
HBV	HBV-F1	TAGCGCCTCATTTTGTGGGT
	HBV-R1	CTTCCTGTCTGGCGATTGGT
	HBV-F2	TAGGACCCCTGCTCGTGTTA
	HBV-R2	CCGTCCGAAGGTTTGGTACA
	HBV-F3	ATGTGGTATTGGGGGCCAAG
	HBV-R3	GGTTGCGTCAGCAAACACTT
	HBV-F4	TGGAACCTTTTCGGCTCCTC
	HBV-R4	GGGAGTCCGCGTAAAGAGAG
	HBV-F6	TACTGCACTCAGGCAAGCAA
	HBV-R6	TGCGAATCCACACTCCGAAA
	HBV-F8	AGACGAAGGTCTCAATCGCC
	HBV-R8	ACCCACAAAATGAGGCGCTA
Mitochondrial DNA	Fw_huND1	CCCTACTTCTAACCTCCCTGTTCTTAT
	Rw_huND1	CATAGGAGGTGTATGAGTTGGTCGTA
	Fw_huND5	ATTTTATTTCTCCAACATACTCGGATT
	Rw_huND5	GGGCAGGTTTTGGCTCGTA
	Fw_huATP6	CATTTACACCAACCACCCAACTATC
	Rw-huATP6	CGAAAGCCTATAATCACTGTGCC

Tables S2: Specific probes of the IAR gene set for multiplexed gene profiling analysis.

Gene	Accession Number	Target Sequence	Note
ATP5B	NM_001686.3	GAAATTCTGGTGACTGGTATCAAGGTTGTCGATCTGCTA GCTCCCTATGCCAAGGGTGGCAAAATTGGGCTTTTTGGT GGTGCTGGAGTTGGCAAGACTG	HG
BAG6	NM_001199698.1	CATTGATCACGGGGCTAGAAGAGTATGTGCGGGAGAGTT TTTCCTTGGTGCAGGTTCAGCCAGGTGTGGACATCATCC GGACAAACCTGGAATTTCTCCA	HG
NDUFA2	NM_001185012.1	ATGGGCTAGGCTTTAGGGTCCGCGGTTGGTCAGACCGG AGCACTTGGCCTGAAGACCTGGAATTGGCGACTTCGATA TTAACAAGGATGGCGGCGGCCGC	HG
ARL9	NM_206919.1	CAGATATCCATGAAGCTTTGGCATTATCTGAAGTGGGAAA TGACAGGAAGATGTTCTTGTTTGGAACCTACCTGACTAAG AATGGCTCAGAGATACCCTC	Schoggins
CASP1	NM_001223.3	TGGAGACATCCCACAATGGGCTCTGTTTTTATTGGAAGA CTCATTGAACATATGCAAGAATATGCCTGTTCCTGTGATG TGGAGGAAATTTTCCGCAAGG	Schoggins
CXCL16	NM_001100812.1	CCATGGGTTCAGGAATTGATGAGCTGTCTTGATCTCAAA GAATGTGGACATGCTTACTCGGGGATTGTGGCCCACCAG AAGCATTTACTTCCTACCAGCC	Schoggins
CXCL8	NM_000584.2	ACAGCAGAGCACACAAGCTTCTAGGACAAGAGCCAGGAA GAAACCACCGGAAGGAACCATCTCACTGTGTGTAAACAT GACTTCCAAGCTGGCCGTGGCT	Schoggins
HERC5	NM_016323.2	TGGGCTGCTGTTTACTTTCGGTGCTGGAAAACATGGGCA ACTTGGTCATAATTCAACACAGAATGAGCTAAGACCCTGT TTGGTGGCTGAGCTTGTTGGG	Schoggins

HERC6	NM_001165136.1	TCCATCACCCAGATTTATACTTAGAGTCAGACGAAGTCGC CTGGTTAAAGATGCTCTGCGTCAATTAAGTCAAGCTGAA GCTACTGACTTCTGCAAAGTA	Schoggins
HLA-B	NM_005514.6	CCCTGAGATGGGAGCCGTCTTCCCAGTCCACCGTCCCC ATCGTGGGCATTGTTGCTGGCCTGGCTGTCCTAGCAGTT GTGGTCATCGGAGCTGTGGTCGC	Schoggins
HLA-H	NR_001434.3	GAGCGGGAGGGGCCGGAGTATTGGGACCGGAACACACA GATCTGCAAGGCCCAAGCACGGACTGAACGAGAGAACC TGCGGATCGCGCTCCGCTACTACA	Schoggins
IFI35	NM_005533.3	TGCCCTCTGCTTGCGGGCTCTGCTCTGATCACCTTTGAT GACCCCAAAGTGGCTGAGCAGGTGCTGCAACAAAAGGA GCACACGATCAACATGGAGGAGT	Schoggins
IFI44	NM_006417.4	GATGAAAGAAAGATAAAAGGGGTCATTGAGCTCAGGAAG AGCTTACTGTCTGCCTTGAGAACTTATGAACCATATGGAT CCCTGGTTCAACAAATACGAA	Schoggins
IFIH1	NM_022168.2	GCTTGGGAGAACCCTCTCCCTTCTCTGAGAAAGAAAGAT GTCGAATGGGTATTCCACAGACGAGAATTTCCGCTATCT CATCTCGTGCTTCAGGGCCAGG	Schoggins
IFIT3	NM_001031683.2	CGCCTGCTAAGGGATGCCCCTTCAGGCATAGGCAGTATT TTCCTGTCAGCATCTGAGCTTGAGGATGGTAGTGAGGAA ATGGGCCAGGGCGCAGTCAGCT	Schoggins
ISG20	NM_002201.5	AGCCCGCCGAGGGCTGCCCCGCCTGGCTGTGTCAGACT GAAGCCCCATCCAGCCCGTTCCGCAGGGACTAGAGGCT TTCGGCTTTTTGGGACAGCAACTA	Schoggins
LRRC17	NM_001031692.1	CAGCACAACCAGATCAAAGTCTTGACGGAGGAAGTGTTC ATTTACACACCTCTCTTGAGCTACCTGCGTCTTTATGACA ACCCCTGGCACTGTACTTGTG	Schoggins
MX1	NM_002462.2	GCCTTTAATCAGGACATCACTGCTCTCATGCAAGGAGAG GAAACTGTAGGGGAGGAAGACATTCGGCTGTTTACCAGA CTCCGACACGAGTTCCACAAAT	Schoggins
OAS2	NM_016817.2	TGAAAAACAATTTCGAGATCCAGAAGTCCCTTGATGGGTT CACCATCCAGGTGTTCACAAAAAATCAGAGAATCTCTTTC GAGGTGCTGGCCGCCTTCAA	Schoggins
OASL	NM_198213.1	GGCGTTTCTGAGCTGTTTCCACAGCTTCCAGGAGGCAGC CAAGCATCACAAAGATGTTCTGAGGCTGATATGGAAAAC CATGTGGCAAAGCCAGGACCTG	Schoggins
PLCG2	NM_002661.2	GCTTGAAAATCTTACACCAGGAAGCGATGAATGCGTCCA CGCCCACCATTATCGAGAGTTGGCTGAGAAAGCAGATAT ATTCTGTGGATCAAACCAGAAG	Schoggins
PSMB8	NM_004159.4	ACTCACAGAGACAGCTATTCTGGAGGCGTTGTCAATATG TACCACATGAAGGAAGATGGTTGGGTGAAAGTAGAAAGT ACAGATGTCAGTGACCTGCTGC	Schoggins
PSMB9	NM_002800.4	TCAGGTATATGGAACCCTGGGAGGAATGCTGACTCGACA GCCTTTTGCCATTGGTGGCTCCGGCAGCACCTTTATCTA TGGTTATGTGGATGCAGCATAT	Schoggins
RARRES3	NM_004585.3	CTGACCCTCGTGCCCTGTCTCAGGCGTTCTCTAGATCCT TTCCTCTGTTTCCCTCTCTCGCTGGCAAAAGTATGATCTA ATTGAAACAAGACTGAAGGAT	Schoggins
SLC15A3	NM_016582.1	GCCGCTTCTTCAACTGGTTTTACTGGAGCATCAACCTGG GTGCTGTGCTGTCGCTGCTGGTGGTGGCGTTTATTCAGC AGAACATCAGCTTCCTGCTGGG	Schoggins
TNFRSF1B	NM_001066.2	CCCAGCTGAAGGGAGCACTGGCGACTTCGCTCTTCCAGT TGGACTGATTGTGGGTGTGACAGCCTTGGGTCTACTAAT AATAGGAGTGGTGAACTGTGTC	Schoggins
UBA7	NM_003335.2	GCGGGAGGATGGGTCCCTGGAGATTGGAGACACAACAA CTTTCTCTCGGTACTTGCGTGGTGGGGCTATCACTGAAG TCAAGAGACCCAAGACTGTGAGA	Schoggins
UBE2L6	NM_004223.3	TGTTTCAAAACCACTTGCCATCCTGTTAGATTGCCAGTTC CTGGGACCAGGCCTCAGACTGTGAAGTATATATCCTCCA GCATTCAGTCCAGGGGGAGCC	Schoggins
ZC3HAV1	NM_020119.3	CTCCTTCTTCACATCGTAGAAACATGGCATATAGGGCTAG AAGCAAGAGTAGAGATCGGTTCTTTCAGGGCAGCCAAGA ATTTCTTGCGTCTGCTTCAGC	Schoggins
ZMYND15	NM_032265.1	CCTCAGAGCGGCCGACAACTGCATGTCCTGGTACTGCAA TGCCTTCATCTTCCACCTGGTTTACAAGCCTGCTCAAGG GAGCGGGGCCCGCCCGGCGCCC	Schoggins

PMAIP1	NM_021127.2	CTAGTGTTTTTGCCGAAGATTACCGCTGGCCTACTGTGA AGGGAGATGACCTGTGATTAGACTGGGCGGCTGGGGAG AAACAGTTCAGTGCATTGTTGTT	Schoggins
GBP4	NM_052941.4	TTCTACAAGATATGCCATGGGCCTTTTCACAGGGGACAC AGGCTTCTTAAAACAACCCGGCTTCCTCACCCTATGTCCT TTATTTACAAAGCTGTGCTCC	Schoggins
TMEM173	NM_198282.1	CTGGCATGGTCATATTACATCGGATATCTGCGGCTGATC CTGCCAGAGCTCCAGGCCCGGATTCGAACTTACAATCAG CATTACAACAACCTGCTACGGG	STING
IFI16	NM_005531.1	ACGACTGAACACAATCAACTGTGAGGAAGGAGATAAACT GAAACTCACCAGCTTTGAATTGGCACCGAAAAGTGGGAA TACCGGGGAGTTGAGATCTGTA	
IFNB1	NM_002176.2	ACAGACTTACAGGTTACCTCCGAAACTGAAGATCTCCTA GCCTGTGCCTCTGGGACTGGACAATTGCTTCAAGCATTC TTCAACCAGCAGATGCTGTTTA	
IRF3	NM_001571.5	TCATGGCCCCAGGACCAGCCGTGGACCAAGAGGCTCGT GATGGTCAAGGTTGTGCCCACGTGCCTCAGGGCCTTGG TAGAAATGGCCCGGGTAGGGGGTG	
IRF7	NM_001572.3	CGCAGCGTGAGGGTGTGTCTTCCCTGGATAGCAGCAGC CTCAGCCTCTGCCTGTCCAGCGCCAACAGCCTCTATGAC GACATCGAGTGCTTCCTTATGGA	
STAT1	NM_139266.1	ACAGTGGTTAGAAAAGCAAGACTGGGAGCACGCTGCCAA TGATGTTTCATTTGCCACCATCCGTTTTCATGACCTCCTG TCACAGCTGGATGATCAATAT	
TBK1	NM_013254.2	ACCAGTCTTCAGGATATCGACAGCAGATTATCTCCAGGT GGATCACTGGCAGACGCATGGGCACATCAAGAAGGCAC TCATCCGAAAGACAGAAATGTAG	

HG: Housekeeping genes
Schoggins: cGAS-related genes described by Shoggins et al., (3)

Supplementary References

1. Verrier ER, Colpitts CC, Bach C, Heydmann L, Weiss A, Renaud M, Durand SC, et al. A targeted functional RNAi screen uncovers Glypican 5 as an entry factor for hepatitis B and D viruses. Hepatology 2016;63:35–48.
2. Lucifora J, Salvetti A, Marniquet X, Mailly L, Testoni B, Fusil F, Inchauspe A, et al. Detection of the hepatitis B virus (HBV) covalently-closed-circular DNA (cccDNA) in mice transduced with a recombinant AAV-HBV vector. Antiviral Res 2017;145:14-19.
3. Schoggins JW, MacDuff DA, Imanaka N, Gainey MD, Shrestha B, Eitson JL, Mar KB, et al. Pan-viral specificity of IFN-induced genes reveals new roles for cGAS in innate immunity. Nature 2014;505:691-695.